

# **An Interactive Shader for Natural Diffraction Gratings**

## **Bachelorarbeit**

der Philosophisch-naturwissenschaftlichen Fakultät  
der Universität Bern

vorgelegt von

Michael Single

2014

Leiter der Arbeit:  
Prof. Dr. Matthias Zwicker  
Institut für Informatik und angewandte Mathematik

## Abstract

In nature color production is the result of physical interaction of light with a surface's nanostructure. In his pioneering work, Stam developed limited reflection models based on wave optics, capturing the effect of diffraction on very regular surface structures. We propose an adaption of his BRDF model such that it can handle complex natural gratings. On top of this, we describe a technique for interactively rendering diffraction effects, as a result of physical interaction of light with biological nanostructures such as snake skins. As input data, our method uses discrete height fields of natural gratings acquired by using atomic force microscopy (AFM). Based on Taylor Series approximation we leverages precomputation to achieve interactive rendering performance (about 5-15 fps). We demonstrate results of our approach using surface nanostructures of different snake species applied on a measured snake geometry. Lastly, we evaluate the quality of our method by a comparison of the maxima for peak viewing angles using the data produced by our method against the maxima resulting by the grating equation.

# Contents

<b>1</b>	<b>Derivations</b>	<b>1</b>
1.1	Problem Statement and Challenges . . . . .	1
1.2	Approximate a FT by a DFT . . . . .	2
1.2.1	Reproduce FT by DTFT . . . . .	2
1.2.2	Spatial Coherence and Windowing . . . . .	3
1.2.3	Reproduce DTFT by DFT . . . . .	5
1.3	Adaption of Stam's BRDF discrete height fields . . . . .	7
1.3.1	Rendering Equation . . . . .	7
1.3.2	Reflected Radiance of Stam's BRDF . . . . .	8
1.3.3	Relative Reflectance . . . . .	9
1.4	Optimization using Taylor Series . . . . .	11
1.5	Spectral Rendering . . . . .	13
1.6	Alternative Approach . . . . .	13
1.6.1	PQ factors . . . . .	13
1.6.2	Interpolation . . . . .	16
<b>2</b>	<b>Implementation</b>	<b>17</b>
2.1	Precomputations in Matlab . . . . .	18
2.2	Java Renderer . . . . .	22
2.3	GLSL Diffraction Shader . . . . .	23
2.3.1	Vertex Shader . . . . .	23
2.3.2	Fragment Shader . . . . .	27
2.4	Technical details . . . . .	31
2.4.1	Texture lookup . . . . .	31
2.4.2	Texture Blending . . . . .	33
2.4.3	Color Transformation . . . . .	33
2.5	Discussion . . . . .	34
<b>A</b>	<b>Signal Processing Basics</b>	<b>36</b>
A.1	Fourier Transformation . . . . .	36
A.2	Convolution . . . . .	38
A.3	Taylor Series . . . . .	38
<b>B</b>	<b>Summary of Stam's Derivations</b>	<b>39</b>

<b>C Derivation Steps in Detail</b>	<b>42</b>
C.1 Taylor Series Approximation . . . . .	42
C.1.1 Proof Sketch of 1. . . . .	42
C.1.2 Part 2: Find such an N . . . . .	42
C.2 PQ approach . . . . .	44
C.2.1 One dimensional case . . . . .	44
C.2.2 Two dimensional case . . . . .	45
<b>D Miscellaneous Transformations</b>	<b>47</b>
D.1 Fresnel Term - Schlick's approximation . . . . .	47
D.2 Spherical Coordinates and Space Transformation . . . . .	47
D.3 Tangent Space . . . . .	48
<b>List of Tables</b>	<b>49</b>
<b>List of Figures</b>	<b>49</b>
<b>List of Algorithms</b>	<b>50</b>
<b>Bibliography</b>	<b>51</b>

# Chapter 1

## Derivations

### 1.1 Problem Statement and Challenges

The goal of this thesis is to perform a physically accurate and interactive simulation of structural colors production like shown in figure 1.2, which we can see whenever a light source is diffracted on a natural grating. For this purpose we need to be provided by the following input data as shown in figure 1.1:

- A mesh representing a snake surface<sup>1</sup> with associated texture coordinates as shown in figure 1.1(a).
- A natural diffraction grating represented as a height field, its maximum height and its pixel-width-correspondence<sup>2</sup>.
- A vectorfield which describes how fingers on a provided surface of the nanostructure are aligned as shown in figure 1.1(c).

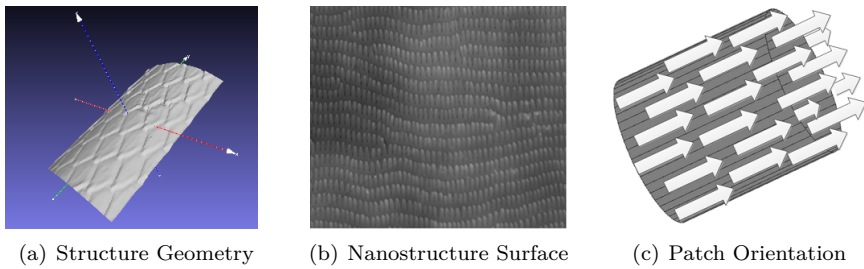


Figure 1.1: Input for our simulation

We want to rely on the integral equation ?? derived by J. Stam in his paper [Sta99] about diffraction shaders. This equation formaltes a BRDF modeling the effect of diffraction under the assumption that a given grating can either be formulated as an analytical function or its structure is

---

<sup>1</sup>Which is in our simulation an actual reconstruction of a real snake skin. These measurements are provided by the Laboratory of Artificial and Natural Evolution at Geneva. See their website: [www.lanevol.org](http://www.lanevol.org).

<sup>2</sup>Since the nanostructure is stored as a grayscale image, we need a scale telling us what length and height one pixel corresponds to in this provided image.

simple enough being modeled relying on statistical methods. These assumptions guarantee that ?? has an explicit solution. However, the complexity of a biological nanostructures cannot sufficiently and accurately modeled simply using statistical methods. This is why interactive computation at high resolution becomes a hard task, since we cannot evaluate the given integral equation on the fly. Therefore, we have to adapt Stam's equation such that we are able to perform interactive rendering using explicitly provided height fields.

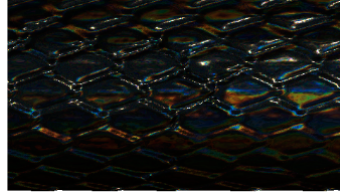


Figure 1.2: Output: Rendered Structural Colors

## 1.2 Approximate a FT by a DFT

### 1.2.1 Reproduce FT by DTFT

In the previous section, we have found an identity for the reflected spectral radiance  $L_\lambda(\omega_r)$  when using Stam's BRDF for a given input height field. However, the derived expression in equation 1.13 requires to evaluate the Fourier Transform of our height field<sup>3</sup> for every direction. In this section we explain how to approximate the FT by the DTFT and apply it to our previous derivations. Figure 1.3 graphically shows how to obtain the DTFT from the FT for a one dimensional signal<sup>4</sup>

The first step is to uniformly discretize the given signal since computers are working finite, discrete arithmetic. We rely on the Nyquist–Shannon sampling theorem tells us how dense we have to sample a given signal  $s(x)$  such that can be reconstructed its sampled version  $\hat{s}[n]$ <sup>6</sup>. In particular, a sampled version according to the Nyquist–Shannon sampling theorem will have the same Fourier Transform as its original signal. The sampling theorem states that if  $f_{max}$  denotes the highest frequency of  $s(x)$ , then, it has to be sampled by a rate of  $f_s$  with  $2f_{max} \leq f_s$  in order to be reconstructable. By convention  $T = \frac{1}{f_s}$  represent the interval length between two samples.

Next, we apply the Fourier Transformation operator on the discretized signal  $\hat{s}$  which gives us the following expression:

<sup>3</sup>actually it requires the computation of the inverse Fourier Transform of a transformed version of the given heightfield, the function  $p(x,y)$  defined in equation ??.

<sup>4</sup>For our case we are dealing with a two dimensional, spatial signal, the given height field. Nevertheless, without any constraints of generality, the explained approach applies to multi dimensional problems.

<sup>5</sup>Images of function plots taken from [http://en.wikipedia.org/wiki/Discrete\\_Fourier\\_transform](http://en.wikipedia.org/wiki/Discrete_Fourier_transform) and are modified.

<sup>6</sup> $n$  denotes the number of samples.

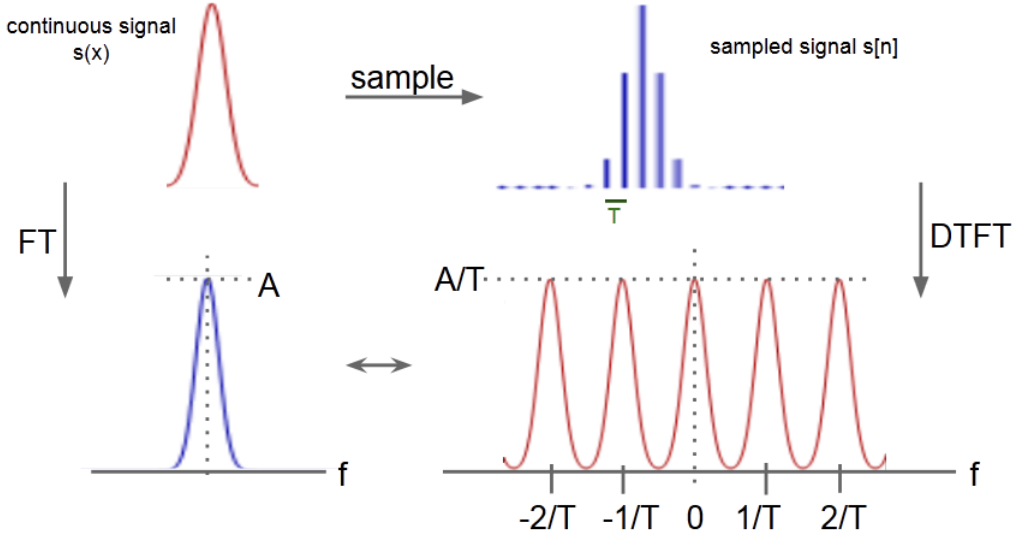


Figure 1.3: Illustration of how to approximate the analytical Fourier Transform (FT) <sup>5</sup> of a given continuous signal by a Discrete Time Fourier Transform (DTFT). The DTFT applied on a band-limited, discretized signal yields a continuous, periodic response in frequency space.

$$\begin{aligned}
 \mathcal{F}_{FT}\{\hat{s}\}(w) &= \int_{\mathbb{R}} \hat{s}[n]e^{-iwx}dx \\
 &= \int_{\mathbb{R}} \text{mask}(x)s(x)e^{-iwx}dx \\
 &= T \sum_{x=-\infty}^{\infty} \hat{s}[x]e^{-iwx} \\
 &= T\mathcal{F}_{DTFT}\{s\}(w)
 \end{aligned} \tag{1.1}$$

Equation 1.1 tells us that if  $\hat{s}$  is sufficiently sampled, then its DTFT corresponds to the FT of  $s(x)$ . Notice that the resulting DTFT from the sampled signal has a height of  $\frac{A}{T}$  where  $A$  is the height of the FT of  $s$  and thus is a scaled version of the FT.

For a given height field  $h$ , let us compute Stam's auxiliary function  $p$  defined as in equation ???. For the reminder of this thesis we introduce the following definition:

$$P_{dtft} \equiv \mathcal{F}_{DTFT}\{p\} \tag{1.2}$$

Therefore  $P_{dtft}$  denotes the DTFT of a transformed version of our height field  $h$ <sup>7</sup>.

### 1.2.2 Spatial Coherence and Windowing

Before we can derive a final expression in order to approximate a FT by a DFT, we first have to revisit the concept of coherence introduced in section ?? of chapter 2. Previously we have seen

<sup>7</sup>By transformed height field we mean  $p(x, y) = e^{i\frac{2\pi}{\lambda}wh(x, y)}$  which we get, when plugging in  $h$  into equation ??? and this expression again plug into equation ???

that Stam's BRDF tells us what is the total contribution of all secondary sources which allows us to say what is the reflected spectral radiance at a certain point in space. This is related to stationary interference which itself depends on the coherence property of the emitted secondary wave sources. The ability for two points in space,  $t_1$  and  $t_2$ , to interfere in the extend of a wave when being averages over time is the so called spatial coherence. The spatial distance between such two points over which there is significant interference is limited by the quantity coherence area. For filtered sunlight on earth this is equal to  $65\mu m$ <sup>8</sup>.

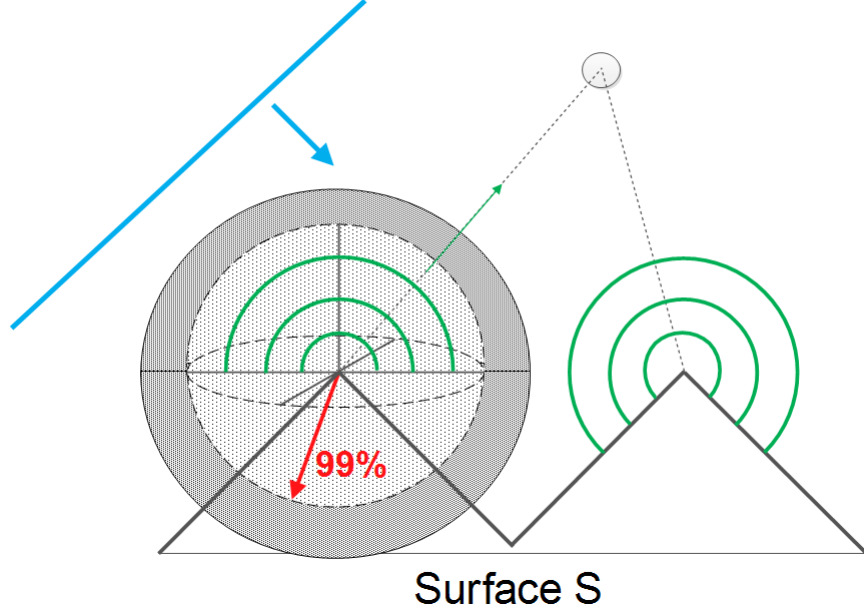


Figure 1.4: A plane wave encounters a surface. According to Huygens principle, secondary wavelets are emitted off from this surface. The resulting wave at a certain point in space (here indicated by a gray circle) depends on the interference among all waves encountering at this position. The amount of significant interference is directly affected by the spatial coherence property of all the wavelets.

Figure 1.4 illustrates the concept of spatial coherence. A wavefront (blue line) encounters a surface. Due to Hugen's Principle, secondary wavelets are emitted off from the surface. The reflected radiance at a certain point in space, e.g. at a viewer's eye position (denoted by the gray circle), is a result of interference among all wavelets at that point. This interference is directly affected by the spatial coherence property of all the emitted wavelets.

In physics spatial coherence is predicted by the cross correlation between  $t_1$  and  $t_2$  and usually modeled by by a Gaussian Random Process. For any such Gaussian Processes we can use a spatial gaussian window  $g(x)$  which is equal:

$$g(x) = \frac{1}{\sqrt{2\pi} \cdot \sigma} \cdot e^{-\frac{x^2}{2\sigma^2}} \quad (1.3)$$

<sup>8</sup>A proof for this number can be looked up in the book Optical Coherence and Quantum Optics[LM95] on page 153 and 154.



We have chosen standard deviation  $\sigma_s$  of the window such that it fulfills the equation  $4\sigma_s = 65\mu\text{m}$ . This is equivalent like saying we want to predict about 99.99%<sup>9</sup> of the resulting spatial coherence interference effects in our model by a cross correlation function.

By applying the Fourier Transformation to the spatial window we get the corresponding window in frequency space will look like:

$$G(f) = e^{-\frac{f^2}{2\sigma_f^2}} \quad (1.4)$$

Notice that this frequency space window has a standard deviation  $\sigma_f$  equal to  $\frac{1}{2\pi\sigma_s}$ . Those two windows, the spatial- and the frequency space window, will be used in the next section in order to approximate the DTFT by the DFT by a windowing approach.

### 1.2.3 Reproduce DTFT by DFT

In this section we explain how and under what assumptions the DTFT of a discretized signal<sup>10</sup> can be approximated by a DFT. The whole idea how to reproduce the DTFT by DFT is schematically illustrated in figure 1.5.

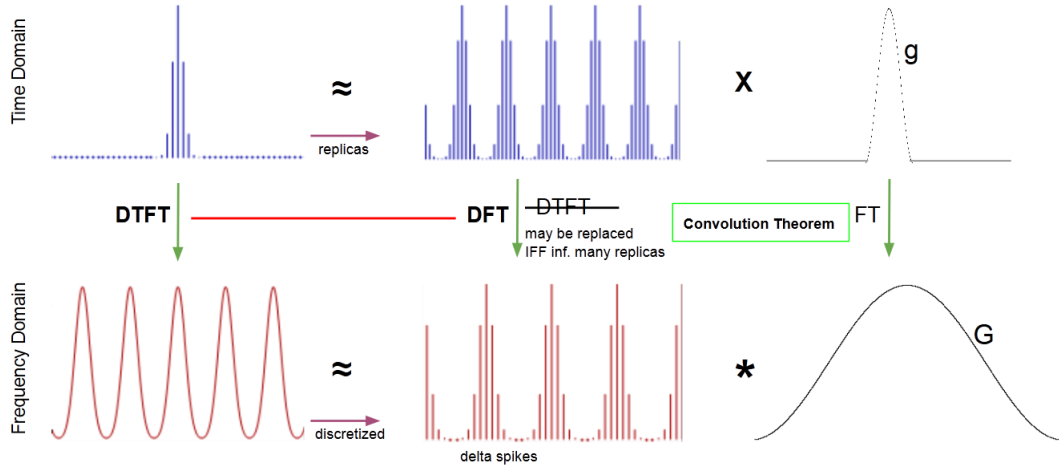


Figure 1.5: Illustration of how to approximate the DTFT<sup>11</sup> by the DFT relying on the Convolution Theorem, using a gaussian window function.

Given a spatial, bandlimited and discretized one dimensional signal  $\hat{s}$ . Our goal is to approximate this spatial signal in a way such that when taking the DTFT of this approximated signal, it will yield almost the same like taking the DTFT of the original sampled  $\hat{s}$ . For this purpose we will use the previous introduced concept of gaussian windows and the so called Convolution Theorem which is a fundamental property of all Fourier Transformations.

<sup>9</sup>Standard deviation values from confidence intervals table of normal distribution provided by Wolfram MathWorld <http://mathworld.wolfram.com/StandardDeviation.html>.

<sup>10</sup>E.g. a sampled signal like already presented in figure 1.3

<sup>11</sup>Images of function plots taken from [http://en.wikipedia.org/wiki/Discrete\\_Fourier\\_transform](http://en.wikipedia.org/wiki/Discrete_Fourier_transform) and are modified. Note that the scales in the graphic are not appropriate.

The Convolution Theorem states that the Fourier Transformation of a product of two functions,  $f$  and  $g$ , is equal to convolving the Fourier Transformations of each individual function. Mathematically, this statement corresponds to equation 1.5:

$$\mathcal{F}\{f \cdot g\} = \mathcal{F}\{f\} * \mathcal{F}\{g\} \quad (1.5)$$

The principal issue is how to approximate our given signal  $\hat{s}$ . Therefore, let us consider another signal  $\hat{s}_N$  which is the  $N$  times replicated version of  $\hat{s}$  (blue signal at center top in figure).

Remember that in general, the signal response at a certain point in space is the result of interference among all signals meeting at that position. In our scenario, the source of those signals are emitted secondary wavelets. The interference strength between these points is related to their spatial coherence. Windowing the signals by a gaussian window  $g$  will capture a certain percentage of all interference effects. From the previous section 1.2.2 we know that we can use gaussian window like in equation 1.3 in order to approximate such spatial signals interference effects.

Using this insight, we can approximate  $\hat{s}$  by taking the product of  $\hat{s}_N$  with a gaussian window  $g$ . This fact is illustrated in the first row of figure 1.3. So what will the DTFT of this approximation yield? We already know that the DTFT of  $\hat{s}$  is a continuous, periodic signal, since  $\hat{s}$  is bandlimited. Thus, taking the DTFT of this found approximation should give us approximately the same continuous, periodic signal.

This is where the convolution theorem comes into play: Applying the DTFT to the product of  $\hat{s}_N$  and  $g$  is the same as convolving the DTFT of  $\hat{s}_N$  by DTFT of  $g$ . From equation 1.4 we already know that the DTFT of  $g$  is just another gaussian, denoted by  $G$ . On the other hand the DTFT of  $\hat{s}_N$  yields a continuous, periodic signal. The higher the value of  $N$ , the sharper the signal gets (denoted by delta spiked) and the closer it converges toward to the DFT. This is why the DFT is the limit of a DTFT applied on periodic and discrete signals. Therefore, for a large number of  $N$  we can replace the DTFT by the DFT operator when applied on  $\hat{s}_N$ .

Lastly, we see that the DTFT of  $\hat{s}$  is approximately the same like convolving a gaussian window by the DFT of  $\hat{s}_N$ . This also makes sense, since convolving a discrete, periodic signal (DFT of  $\hat{s}_N$ ) by a continuous window function  $G$  yields a continuous, periodic function.

In practise, we cannot compute the DTFT A.3 numerically due to finite computer arithmetic and hence working with the DFT is our only option. Furthermore, there are numerically fast algorithms in order to compute the DFT values of a function, the Fast Fourier Transformation (FFT). The DFT A.4 of a discrete height field is equal to the DTFT of an infinitely periodic function consisting of replicas of the same height field. Not, let a spatial gaussian window  $g$  having a standard deviation for which  $4\sigma_s$  is equal  $\mu m$ . Then, from before, it follows:

$$\mathcal{F}_{dft}\{\mathbf{s}\} \equiv \mathcal{F}_{dft}\{\mathbf{s}\} * G(\sigma_f) \quad (1.6)$$

Therefore we can deduce the following expression from this:

$$\begin{aligned}
\mathcal{F}_{dft}\{\mathbf{t}\}(u, v) &= \int_{-\infty}^{\infty} \int_{-\infty}^{\infty} F_{dft}\{\mathbf{t}\}(w_u, w_v) \phi(u - w_u, v - w_v) dw_u dw_v \\
&= \int_{-\infty}^{\infty} \int_{-\infty}^{\infty} \sum_i \sum_j F_{dft}\{\mathbf{t}\}(w_u, w_v) \\
&\quad \delta(w_u - w_i, w_v - w_j) \phi(u - w_u, v - w_v) dw_u dw_v \\
&= \sum_i \sum_j \int_{-\infty}^{\infty} \int_{-\infty}^{\infty} F_{dft}\{\mathbf{t}\}(w_u, w_v) \\
&\quad \delta(w_u - w_i, w_v - w_j) \phi(u - w_u, v - w_v) dw_u dw_v \\
&= \sum_i \sum_j F_{dft}\{\mathbf{t}\}(w_u, w_v) \phi(u - w_u, v - w_v)
\end{aligned} \tag{1.7}$$

where

$$\phi(x, y) = \pi e^{-\frac{x^2 + y^2}{2\sigma_f^2}} \tag{1.8}$$

### 1.3 Adaption of Stam's BRDF discrete height fields

#### 1.3.1 Rendering Equation

As already discussed in the theoretical background chapter, colors are associated to radiance. Since we are starting with Stam's BRDF<sup>12</sup> formulation but want to perform a simulation rendering structural colors, we have to reformulate this BRDF equation such that we will end up with an identity of the reflected spectral radiance. This is where the rendering equation comes into play. Lets assume we have given an incoming light source with solid angle  $\omega_i$  and  $\theta_i$  is its angle of incidence,  $\omega_r$  is the solid angle for the reflected light. Further let  $\lambda$  denote the wavelength<sup>13</sup> and  $\Omega$  is the hemisphere of integration for the incoming light. Then, we are able to formulate a  $BRDF_\lambda$  by using its definition ??:

$$\begin{aligned}
f_r(\omega_i, \omega_r) &= \frac{dL_r(\omega_r)}{L_i(\omega_i) \cos(\theta_i) d\omega_i} \\
\Rightarrow f_r(\omega_i, \omega_r) L_i(\omega_i) \cos(\theta_i) d\omega_i &= dL_r(\omega_r) \\
\Rightarrow \int_{\Omega} f_r(\omega_i, \omega_r) L_i(\omega_i) \cos(\theta_i) d\omega_i &= \int_{\Omega} dL_r(\omega_r) \\
\Rightarrow \int_{\Omega} f_r(\omega_i, \omega_r) L_i(\omega_i) \cos(\theta_i) d\omega_i &= L_r(\omega_r)
\end{aligned} \tag{1.9}$$

The last equation is the so called rendering equation . We assume that our incident light is a directional, unpolarized light source like sunlight and therefore its radiance is given as

$$L_\lambda(\omega) = I(\lambda) \delta(\omega - \omega_i) \tag{1.10}$$

<sup>12</sup>Remember that a BRDF is the portion of a incident light source reflected off a given surface towards a specified viewing direction.

<sup>13</sup>Notice that, to keep our terms simple, we have dropped all  $\lambda$  subscripts for spectral radiance quantites.

where  $I(\lambda)$  is the intensity of the relative spectral power for the wavelength  $\lambda$ . By plugging the identity in equation 1.10 into our current rendering equation 1.9, we will get:

$$\begin{aligned} L_\lambda(\omega_r) &= \int_{\Omega} BRDF_\lambda(\omega_i, \omega_r) L_\lambda(\omega_i) \cos(\theta_i) d\omega_i \\ &= BRDF_\lambda(\omega_i, \omega_r) I(\lambda) \cos(\theta_i) \end{aligned} \quad (1.11)$$

where  $L_\lambda(\omega_i)$  is the incident radiance and  $L_\lambda(\omega_r)$  is the radiance reflected by the given surface. Note that the integral in equation 1.11 vanishes since  $\delta(\omega - \omega_i)$  is only equal one if and only if  $\omega = \omega_i$ .

### 1.3.2 Reflected Radiance of Stam's BRDF

We are going to use Stam's main derivation (??) for the  $BRDF(\omega_i, \omega_r)$  in 1.11 by applying the fact that the wavenumber is equal  $k = \frac{2\pi}{\lambda}$ :

$$\begin{aligned} BRDF(\omega_i, \omega_r) &= \frac{k^2 F^2 G}{4\pi^2 A w^2} \langle |P(ku, kv)|^2 \rangle \\ &= \frac{4\pi^2 F^2 G}{4\pi^2 A \lambda^2 w^2} \langle |P(ku, kv)|^2 \rangle \\ &= \frac{F^2 G}{A \lambda^2 w^2} \left\langle \left| P\left(\frac{2\pi u}{\lambda}, \frac{2\pi v}{\lambda}\right) \right|^2 \right\rangle \end{aligned} \quad (1.12)$$

Going back to equation 1.11 and plugging equation 1.12 into it, using the definition of equation ?? and the equation D.2 for  $\omega$  we will get the following:

$$\begin{aligned} L_\lambda(\omega_r) &= \frac{F^2 (1 + \omega_i \cdot \omega_r)^2}{A \lambda^2 \cos(\theta_i) \cos(\theta_r) \omega^2} \left\langle \left| P\left(\frac{2\pi u}{\lambda}, \frac{2\pi v}{\lambda}\right) \right|^2 \right\rangle \cos(\theta_i) I(\lambda) \\ &= I(\lambda) \frac{F^2 (1 + \omega_i \cdot \omega_r)^2}{\lambda^2 A \omega^2 \cos(\theta_r)} \left\langle \left| P\left(\frac{2\pi u}{\lambda}, \frac{2\pi v}{\lambda}\right) \right|^2 \right\rangle \end{aligned} \quad (1.13)$$

Note that the Fresnel term  $F$  is actually a function of  $(\omega_i, \omega_r)$ , but in order to keep the equations simple, we omitted its arguments. So far we just plugged Stam's BRDF identity into the rendering equation and hence have not significantly deviated from his formulation. Keep in mind that  $P$  deontes the Fourier transform of the provided height field which depends on the viewing and incidence light direction. Thus this Fourier Transform has to be recomputed for every direction which will slow down the whole computation quite a lot<sup>14</sup>. One particular strategy to solve this issue is to approximate  $P$  by the Discrete Fourier Transform (DFT)<sup>15</sup> and separate its computation such that terms for many directions can be precomputed and then later retrieved by look ups. The approximation of  $P$  happens in two steps: First we approximate the Fourier Transform by the Discrete Time Fourier Transform (DTFT) and then, afterwards, we approximate the DTFT by the DFT. For further about basics of signal processing and Fourier Transformations please consult the appendix A.

<sup>14</sup>Even a fast variant of computation the Fourier Transform has a runtime complexity of  $O(N \log N)$  where  $N$  is the number of sample.

<sup>15</sup>See appendix A for further information about different kinds of fourier transformations.

Using the insight gained by equation 1.1 allows us to further simplify equation 1.13:

$$\begin{aligned} L_\lambda(\omega_r) &= I(\lambda) \frac{F^2(1 + \omega_i \cdot \omega_r)^2}{\lambda^2 A w^2 \cos(\theta_r)} \left\langle \left| P\left(\frac{2\pi u}{\lambda}, \frac{2\pi v}{\lambda}\right) \right|^2 \right\rangle \\ &= I(\lambda) \frac{F^2(1 + \omega_i \cdot \omega_r)^2}{\lambda^2 A w^2 \cos(\theta_r)} \left\langle \left| T^2 P_{dtft}\left(\frac{2\pi u}{\lambda}, \frac{2\pi v}{\lambda}\right) \right|^2 \right\rangle \end{aligned} \quad (1.14)$$

Where  $P_{dtft}$  is a substitute for  $\mathcal{F}_{DTFT}\{s\}(w)$ . Furthermore  $T$  the sampling distance for the discretization of  $p(x, y)$  assuming equal and uniform sampling in both dimensions  $x$  and  $y$ .

### 1.3.3 Relative Reflectance

In this section we are going to explain how to scale our BRDF formulation such that all of its possible output values are mapped into the range  $[0, 1]$ . Such a relative reflectance formulation will ease our life for later rendering purposes since usually color values are within the range  $[0, 1]$ , too. Furthermore, this will allow us to properly blend the resulting illumination caused by diffraction with a texture map.

Let us examine what  $L_\lambda(\omega_r)$  will be for a purely specular surface, for which  $\omega_r = \omega_0 = \omega_i$  such that  $\omega_0 = (0, 0, 1)$ . For this specular reflection case, the corresponding radiance will be denoted as  $L_\lambda^{spec}(\omega_0)$ . When we know the expression for  $L_\lambda^{spec}(\omega_0)$  we would be able to compute the relative reflected radiance for our problem 1.13 by simply taking the fraction between  $L_\lambda(\omega_r)$  and  $L_\lambda^{spec}(\omega_0)$  which is denoted by:

$$\rho_\lambda(\omega_i, \omega_r) = \frac{L_\lambda(\omega_r)}{L_\lambda^{spec}(\omega_0)} \quad (1.15)$$

Notice that the third component  $w$  from the vector in equation ?? is squared equal  $(\cos(\theta_i) + \cos(\theta_r))^{216}$ . But first, let us derive the following expression:

$$\begin{aligned} L_\lambda^{spec}(\omega_0) &= I(\lambda) \frac{F(\omega_0, \omega_0)^2 (1 + \begin{pmatrix} 0 \\ 0 \\ 1 \end{pmatrix} \cdot \begin{pmatrix} 0 \\ 0 \\ 1 \end{pmatrix})^2}{\lambda^2 A (\cos(0) + \cos(0))^2 \cos(0)} \left\langle \left| T_0^2 P_{dtft}(0, 0) \right|^2 \right\rangle \\ &= I(\lambda) \frac{F(\omega_0, \omega_0)^2 (1 + 1)^2}{\lambda^2 A (1 + 1)^2 1} \left| T_0^2 N_{sample} \right|^2 \\ &= I(\lambda) \frac{F(\omega_0, \omega_0)^2}{\lambda^2 A} \left| T_0^2 N_{sample} \right|^2 \end{aligned} \quad (1.16)$$

Where  $N_{samples}$  is the number of samples of the DTFT A.3. Thus, we can plug our last derived expression 1.16 into the definition for the relative reflectance radiance 1.15 in the direction  $\omega_r$  and will get:

---

<sup>16</sup>Consult section D.2 in the appendix

$$\begin{aligned}
\rho_\lambda(\omega_i, \omega_r) &= \frac{L_\lambda(\omega_r)}{L_\lambda^{spec}(\omega_0)} \\
&= \frac{I(\lambda) \frac{F(\omega_i, \omega_r)^2 (1 + \omega_i \cdot \omega_r)^2}{\lambda^2 A (\cos(\theta_i) + \cos(\theta_r))^2 \cos(\theta_r)} \left\langle \left| T_0^2 P_{dft} \left( \frac{2\pi u}{\lambda}, \frac{2\pi v}{\lambda} \right) \right|^2 \right\rangle}{I(\lambda) \frac{F(\omega_0, \omega_0)^2}{\lambda^2 A} \left| T_0^2 N_{sample} \right|^2} \\
&= \frac{F^2(\omega_i, \omega_r) (1 + \omega_i \cdot \omega_r)^2}{F^2(\omega_0, \omega_0) (\cos(\theta_i) + \cos(\theta_r))^2 \cos(\theta_r)} \left\langle \left| \frac{P_{dft} \left( \frac{2\pi u}{\lambda}, \frac{2\pi v}{\lambda} \right)}{N_{samples}} \right|^2 \right\rangle \quad (1.17)
\end{aligned}$$

For simplification and better readability, let us introduce the following expression, the so called gain-factor:

$$C(\omega_i, \omega_r) = \frac{F^2(\omega_i, \omega_r) (1 + \omega_i \cdot \omega_r)^2}{F^2(\omega_0, \omega_0) (\cos(\theta_i) + \cos(\theta_r))^2 \cos(\theta_r) N_{samples}^2} \quad (1.18)$$

Using equation 1.18, we will get the following expression for the relative reflectance radiance from equation 1.17:

$$\rho_\lambda(\omega_i, \omega_r) = C(\omega_i, \omega_r) \left\langle \left| P_{dft} \left( \frac{2\pi u}{\lambda}, \frac{2\pi v}{\lambda} \right) \right|^2 \right\rangle \quad (1.19)$$

Using the previous definition for the relative reflectance radiance equation 1.15:

$$\rho_\lambda(\omega_i, \omega_r) = \frac{L_\lambda(\omega_r)}{L_\lambda^{spec}(\omega_0)} \quad (1.20)$$

Which we can rearrange to the expression:

$$L_\lambda(\omega_r) = \rho_\lambda(\omega_i, \omega_r) L_\lambda^{spec}(\omega_0) \quad (1.21)$$

Let us choose  $L_\lambda^{spec}(\omega_0) = S(\lambda)$  such that it has the same profile as the relative spectral power distribution of CIE Standard Illuminant *D65* discussed in 2.4.3. Furthermore, when integrating over  $\lambda$  for a specular surface, we should get *CIE<sub>XYZ</sub>* values corresponding to the white point for *D65*. The corresponding tristimulus values using CIE colormatching functions ?? for the *CIE<sub>XYZ</sub>* values look like:

$$\begin{aligned}
X &= \int_\lambda L_\lambda(\omega_r) \bar{x}(\lambda) d\lambda \\
Y &= \int_\lambda L_\lambda(\omega_r) \bar{y}(\lambda) d\lambda \\
Z &= \int_\lambda L_\lambda(\omega_r) \bar{z}(\lambda) d\lambda \quad (1.22)
\end{aligned}$$

where  $\bar{x}$ ,  $\bar{y}$ ,  $\bar{z}$  are the color matching functions. Combining our last finding from equation 1.21 for  $L_\lambda(\omega_r)$  with the definition of the tristimulus values from equation 1.22, allows us to derive a formula for computing the colors values using Stam's BRDF formula relying on the rendering equation 1.9. Without any loss of generality it suffices to derive an explicit expression for just one tristimulus term, for example *Y*, the luminance:

$$\begin{aligned}
Y &= \int_{\lambda} L_{\lambda}(\omega_r) \bar{y}(\lambda) d\lambda \\
&= \int_{\lambda} \rho_{\lambda}(\omega_i, \omega_r) L_{\lambda}^{spec}(\omega_0) \bar{y}(\lambda) d\lambda \\
&= \int_{\lambda} \rho_{\lambda}(\omega_i, \omega_r) S(\lambda) \bar{y}(\lambda) d\lambda \\
&= \int_{\lambda} C(\omega_i, \omega_r) \left\langle \left| P_{dft} \left( \frac{2\pi u}{\lambda}, \frac{2\pi v}{\lambda} \right) \right|^2 \right\rangle S(\lambda) \bar{y}(\lambda) d\lambda \\
&= C(\omega_i, \omega_r) \int_{\lambda} \left\langle \left| P_{dft} \left( \frac{2\pi u}{\lambda}, \frac{2\pi v}{\lambda} \right) \right|^2 \right\rangle S(\lambda) \bar{y}(\lambda) d\lambda \\
&= C(\omega_i, \omega_r) \int_{\lambda} \left\langle \left| P_{dft} \left( \frac{2\pi u}{\lambda}, \frac{2\pi v}{\lambda} \right) \right|^2 \right\rangle S_y(\lambda) d\lambda
\end{aligned} \tag{1.23}$$

Where we used the definition  $S_y(\lambda) \bar{y}(\lambda)$  in the last step.

## 1.4 Optimization using Taylor Series

Our final goal is to render structural colors resulting by the effect of wave diffraction. So far, we have derived an expression which can be used for rendering. Nevertheless, our current equation 1.23 used for computing structural colors, cannot directly be used for interactive rendering, since  $P_{dft}$  had to be recomputed for every change in any direction<sup>17</sup>.

In this section, we will address this issue and deliver an approximation for  $P_{dft}$  defined in equation 1.2. This approximation will allow us to separate  $P_{dft}$  in a certain way such that some computational expensive terms can be precomputed. The main idea is to formulate  $P_{dft}$  as a series expansion relying on the definition of Taylor Series, like defined in equation A.8. Further, we will provide an error bound for our approximation approach for a given number of terms. Last, we will plug our finding extend our current BRDF formula from equation 1.23 by the findings derived within this section.

Let us consider  $p(x, y) = e^{ikwh(x, y)}$  from Stam's Paper ?? where  $h(x, y)$  is a given height field and  $k = \frac{2\pi}{\lambda}$  denotes the wavenumber of wavelength  $\lambda$ . For any complex number  $t$  the power series expansion of the exponential function is equal to:

$$e^t = 1 + t + \frac{t^2}{2!} + \frac{t^3}{3!} + \dots = \sum_{n=0}^{\infty} \frac{t^n}{n!} \tag{1.24}$$

Now, when we use the exponent<sup>18</sup> of  $p(x, y)$  as an input argument for equation 1.24 we get:

<sup>17</sup>According to changes in viewing- or incident light direction.

<sup>18</sup>This exponent is a complex valued function, equal to  $ikwh(x, y)$ .

$$\begin{aligned}
e^t &= e^{ikwh} \\
&= 1 + (ikwh) + \frac{1}{2!}(ikwh)^2 + \frac{1}{3!}(ikwh)^3 + \dots \\
&= \sum_{n=0}^{\infty} \frac{(ikwh)^n}{n!}.
\end{aligned} \tag{1.25}$$

where  $i$  is the imaginary unit for complex numbers. For simplification, in the reminder of this section we omitted the arguments of  $h$ . Equation 1.25 gives us an expression for an exponential series expansion for an for the exponent of  $p(x, y)$ . Please note that above's taylor series is convergent for any complex valued number. Therefore the equation 1.25 is equal to

$$p(x, y) = \sum_{n=0}^{\infty} \frac{(ikwh(x, y))^n}{n!} \tag{1.26}$$

and thus gives us a series representation of  $p(x, y)$ . Next, calculating the Fourier Transformation  $\mathcal{F}$  of equation 1.26 gives us the identity:

$$\begin{aligned}
\mathcal{F}\{p\} &\equiv \mathcal{F}\left\{\sum_{n=0}^{\infty} \frac{(ikwh)^n}{n!}\right\} \\
&\equiv \sum_{n=0}^{\infty} \mathcal{F}\left\{\frac{(ikwh)^n}{n!}\right\} \\
&\equiv \sum_{n=0}^{\infty} \frac{(ikw)^n}{n!} \mathcal{F}\{h^n\}
\end{aligned} \tag{1.27}$$

Where we have exploited the fact that the Fourier Transformation is a linear operator. Therefore, in equation 1.27, we have shown that the Fourier Transformation of a series is equal to the sum of the Fourier Transformation, applied on each individual series term. Reusing the identifier  $P^{19}$  in order to determin the Fourier Transformation of Stams definition  $p$  from equation ??, equation 1.27 then correspond to:

$$P(\alpha, \beta) = \sum_{n=0}^{\infty} \frac{(ikw)^n}{n!} \mathcal{F}\{h^n\}(\alpha, \beta) \tag{1.28}$$

Up to now we have found a infinity series representation for  $P_{dtft}$ . Next we are going to look for an upper bound  $N \in \mathbb{N}$  such that

$$\tilde{P}_N(\alpha, \beta) := \sum_{n=0}^N \frac{(ikwh)^n}{n!} \mathcal{F}\{h^n\}(\alpha, \beta) \approx P(\alpha, \beta) \tag{1.29}$$

$\tilde{P}_N$  is a good approximation of  $P$ , i.e. their absolute difference is small<sup>20</sup>. But first, the following two facts would have to be proven<sup>21</sup>:

1. Show that there exist such an  $N \in \mathbb{N}$  s.t. the approximation of equation 1.29 holds true.

<sup>19</sup>This identifier  $P$  may be subscripted by  $dtft$  which will denote the DTFT variant of  $P$ .

<sup>20</sup>Mathematically speaking, this statement correspond to  $\|\tilde{P}_N - P\| \leq \epsilon$ , where  $\epsilon > 0$  is a small number.

<sup>21</sup>Please have a look in section C.1 in the appendix



2. Find a value for  $N$  s.t. this approximation is below a certain error bound, e.g. close to machine precision  $\epsilon$ .

Assuming these facts are proven and there actually exists such an  $N$ , we can make use of the Taylor series approximation from equation 1.29 and use it for approximating  $P_{dft}$ . This idea allows us to adapt equation 1.23, which is used for computing the structural colors of our BRDF model, in numerically fast way. E.g. the equation for the luminance is then be equal:

$$\begin{aligned} Y &= C(w_i, w_r) \int_{\lambda} \left\langle \left| P_{dft}\left(\frac{2\pi u}{\lambda}, \frac{2\pi v}{\lambda}\right) \right|^2 S_y(\lambda) d\lambda \right. \\ &= C(w_i, w_r) \int_{\lambda} \left| \sum_{n=0}^N \frac{(wk)^n}{n!} \mathcal{F}\{i^n h^n\} \left(\frac{2\pi u}{\lambda}, \frac{2\pi v}{\lambda}\right) \right|^2 S_y(\lambda) d\lambda \end{aligned} \quad (1.30)$$

Notice that equation 1.30 is contrainted by  $N$  and hence is an approximation of equation 1.23. Furthermore, it is possible to separete out all the Fourier Terms in the summation and precompute them. This is why the approach in equation 1.30 is fast in order to compute structural color values according to our BRDF model.

## 1.5 Spectral Rendering

As the last step of our series of derivations, we plug all our findings together to one big equation. in order to compute the color for each pixel on our mesh in the  $CIE_{XYZ}$  colorspace. For any given heigh-field  $h(x, y)$  representing a grating of a nano structure and for given direction vectors  $w_i$  and  $w_r$  as shown in figure ?? the resulting color caused by the effect of diffraction can be computed the following way:

$$DFT_n\{h\}(u, v) = F_{dft}\{i^n h^n\}\left(\frac{2\pi u}{\lambda}, \frac{2\pi v}{\lambda}\right) \quad (1.31)$$

$$W_n(u, v) = \sum_{(r,s) \in \mathcal{N}_1(u,v)} |DFT_n\{h\}(u - w_r, v - w_s)|^2 \phi(u - w_r, v - w_s) \quad (1.32)$$

where  $\phi(x, y) = \pi e^{-\frac{x^2+y^2}{2\sigma_f^2}}$  is the Gaussian window from equation 1.23 and  $\mathcal{N}_1(u, v)$  denotes the one-neighborhood around  $(u, v)$ . Then  $\forall(u, v, w)$  like defined in equation ??, our final expression for computing structural colors due to diffraction, using all our previous derivations, will be equal:

$$\begin{pmatrix} X \\ Y \\ Z \end{pmatrix} = C(\omega_i, \omega_r) \int_{\Lambda} \sum_{n=0}^N \frac{(2\pi w)^n}{\lambda^n n!} W_n(u, v) \begin{pmatrix} S_x(\lambda) \\ S_y(\lambda) \\ S_z(\lambda) \end{pmatrix} d\lambda \quad (1.33)$$

## 1.6 Alternative Approach

### 1.6.1 PQ factors

In this section we are presenting an alternative approach to the previous Gaussian window approach 1.2.3 in order to solve the issue working with  $DTFT$  instead the  $DFT$ . We assume, that a given

surface  $S$  is covered by a number of replicas of a provided representative surface patch  $f$ . In a simplified, one dimensional scenario, mathematically speaking,  $f$  is assumed to be a repetitive function, i.e.  $\forall x \in \mathbb{R} : S(x) = S(x + nT)$ , where  $T$  is its period and  $n \in \mathbb{N}_0$ . Thus, the surfaces can be written formally as:

$$S(x) = \sum_{n=0}^N f(x + nT) \quad (1.34)$$

What we are looking for is an identity for the Fourier Transform<sup>22</sup> of our surface  $S$ , required in order to simplify the  $(X, Y, Z)$  colors from 1.30:

$$\begin{aligned} \mathcal{F}\{S\}(w) &= \int f(x)e^{iwx} dx \\ &= \int_{-\infty}^{\infty} \sum_{n=0}^N f(x + nT)e^{iwx} dx \\ &= \sum_{n=0}^N \int_{-\infty}^{\infty} f(x + nT)e^{iwx} dx \end{aligned} \quad (1.35)$$

Next, apply the following substitution  $x + nT = y$  which will lead us to:

$$\begin{aligned} x &= y - nT \\ dx &= dy \end{aligned} \quad (1.36)$$

Plugging this substitution back into equation 1.35 we will get:

$$\begin{aligned} \mathcal{F}\{S\}(w) &= \sum_{n=0}^N \int_{-\infty}^{\infty} f(x + nT)e^{iwx} dx \\ &= \sum_{n=0}^N \int_{-\infty}^{\infty} f(y)e^{iw(y-nT)} dy \\ &= \sum_{n=0}^N e^{-iwnT} \int_{-\infty}^{\infty} f(y)e^{iwy} dy \\ &= \sum_{n=0}^N e^{-iwnT} \mathcal{F}\{f\}(w) \\ &= \mathcal{F}\{f\}(w) \sum_{n=0}^N e^{-iwnT} \end{aligned} \quad (1.37)$$

We used the fact that the exponential term  $e^{-iwnT}$  is a constant factor when integrating along  $dy$  and the identity for the Fourier Transform of the function  $f$ . Next, let us examine the series  $\sum_{n=0}^N e^{-iwnT}$  closer:

---

<sup>22</sup>Remember that we are using the definition of Fourier Transform used in electrical engineering where  $\mathcal{F}$  actually corresponds to the inverse Fourier Transform.

$$\begin{aligned}
\sum_{n=0}^N e^{-uwnT} &= \sum_{n=0}^N (e^{-iwt})^n \\
&= \frac{1 - e^{iwt(N+1)}}{1 - e^{-iwt}}
\end{aligned} \tag{1.38}$$

We recognize the geometric series identity for the left-hand-side of equation 1.38. Mainly relying on trigonometric identities, equation 1.37 can further simplified to:

$$\mathcal{F}\{S\}(w) = (p + iq)\mathcal{F}\{f\}(w) \tag{1.39}$$

where  $p$  and  $q$  are defined like:

$$\begin{aligned}
p &= \frac{1}{2} + \frac{1}{2} \left( \frac{\cos(wTN) - \cos(wT(N+1))}{1 - \cos(wT)} \right) \\
q &= \frac{\sin(wT(N+1)) - \sin(wTN) - \sin(wT)}{2(1 - \cos(wT))}
\end{aligned} \tag{1.40}$$

Please notice, all derivation steps can be found in the appendix in section C.2.1.

Now lets consider our actual problem description. Given a patch of a nanoscaled sureface snake shed represented as a two dimensional heightfield  $h(x, y)$ . We once again assume that this provided patch is representing the whole surface  $S$  of our geometry by some number of replicas of itself. Therefore,  $S(x, y) = \sum_{n=0}^N h(x + nT_1, y + mT_2)$ , assuming the given height field has the dimensions  $T_1$  by  $T_2$ . In order to derive an identity for the two dimensional Fourier transformation of  $S$  we can similarly proceed like we did to derive equation 1.39.

$$\mathcal{F}\{S\}(w_1, w_2) = (p + iq)\mathcal{F}_{DTFT}\{h\}(w_1, w_2) \tag{1.41}$$

Where all derivation steps can be found in the appendix in section C.2.2 and we have defined

$$\begin{aligned}
p &:= (p_1p_2 - q_1q_2) \\
q &:= (p_1p_2 + q_1q_2)
\end{aligned} \tag{1.42}$$

For the identity of equation 1.41 we made use of Green's integration rule which allowed us to split the double integral to the product of two single integrations. Also, we used the definition of the 2-dimensional inverse Fourier transform of the height field function. We applied a similar substitution like we did in 1.36, but this time twice, once for  $x_1$  and once for  $x_2$  separately. The last step in equation 1.41, substituting with  $p$  and  $q$  in equation C.18 will be useful later in the implementation. The insight should be, that the product of two complex numbers is again a complex number. We will have to compute the absolute value of  $\mathcal{F}\{S\}(w_1, w_2)$  which will then be equal  $(p^2 + q^2)^{\frac{1}{2}} |\mathcal{F}\{h\}(w_1, w_2)|$

### 1.6.2 Interpolation

In 1.6.1 we have derived an alternative approach when we are working with a periodic signal instead using the gaussian window approach from 1.2.3. Its main finding 1.41 that we can just integrate over one of its period instead iterating over the whole domain. Nevertheless, this main finding is using the inverse DTFT. Since we are using

We are interested in recovering an original analog signal  $x(t)$  from its samples  $x[n] =$

Therefore, for a given sequence of real numbers  $x[n]$ , representing a digital signal, its correspond continuous function is:

$$x(t) = \sum_{n=-\infty}^{\infty} x[n] \text{sinc} \left( \frac{t - nT}{T} \right) \quad (1.43)$$

which has the Fourier transformation  $X(f)$  whose non-zero values are confined to the region  $|f| \leq \frac{1}{2T} = B$ . When  $x[n]$  represents time samples at interval  $T$  of a continuous function, then the quantity  $f_s = \frac{1}{T}$  is known as its sample rate and  $\frac{f_s}{2}$  denotes the Nyquist frequency. The sampling Theorem states that when a function has a Bandlimit  $B$  less than the Nyquist frequency, then  $x(t)$  is a perfect reconstruction of the original function.

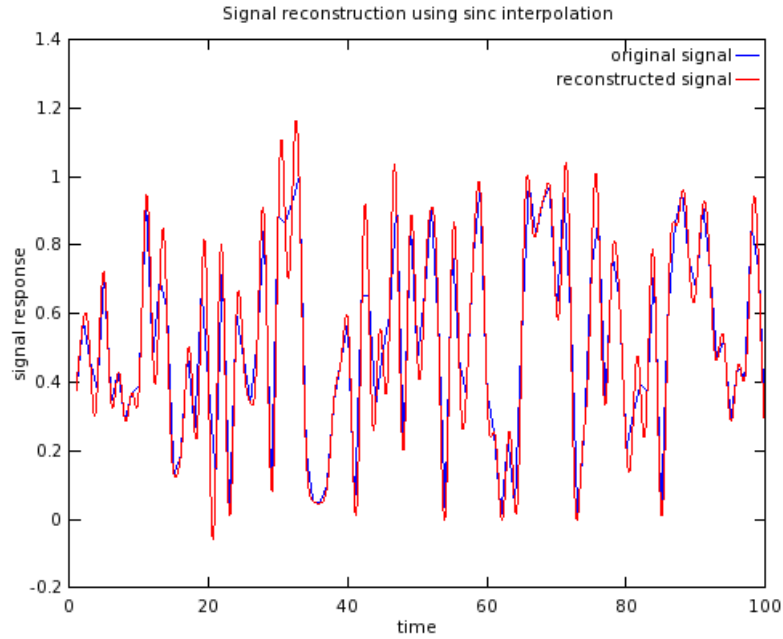


Figure 1.6: Comparisson between a given random one dimensional input signal  $s(t)$  and its sinc interpolation  $\hat{s}(t)$ . Notice that for the interpolation there were  $N = 100$  samples from the original signal provided.

## Chapter 2

# Implementation

In computer graphics, we generally synthesize 2d images from a given 3d scene description<sup>1</sup>. This process is denoted as rendering. A usual computer graphics scene consist of a viewer's eye, modeled by a virtuel camera, light sources and geometries placed in the world<sup>2</sup>, having some material properties<sup>3</sup> assigned to. In our implementation, scene geometries are modeled by triangular meshes for which each triangle is represented by a triple of vertices. Each vertex has a position, a surface normal and a tangent vector associated with.

The process of rendering basically involves a mapping of 3d scene objects to a 2d image plane and the computation of each image pixel's color according to the provided lighting, viewing and material information of the given scene. These pixel colors are computed in several statges in so called shader programs, directly running on the Graphic Processing Unit (GPU) hardware device. In order to interact with a GPU, for our implementations, we rely on the programing interface of OpenGL<sup>4</sup>, a cross-language, multiplatform API. In OpenGL, there are two fundamental shading pipeline stages, the vertex- and the fragment shading stage, each applied sequentially. Vertex shaders apply all transformations to the mesh vertices and pass this data to the fragment shaders. Fragment shaders receive linearly interpolated vertex data of a particular triangle. They are responsible to compute the color of his triangle.

In this chapter we explain in detail a technique for rendering structural colors due to diffraction effects on natural graings, based on the model we have derived in the previous chapter 1, summarized in section 1.5. For this purpose we implemented a reference framework which is based on a class project of the lecture *Computer Graphics* held by Mr. M. Zwicker which I attended in autumn 2012<sup>5</sup>.

For performing the rendering process, our implementation expects being provided by the fol-

---

<sup>1</sup>A usual computer graphics scene consist of a viewer's eye, modeled by a virtuel camera, light sources and geometries placed in the world, having some material properties assigned to.

<sup>2</sup>With the term world we are refering to a global coordinate system which is used in order to place all objects.

<sup>3</sup>Example material properties are: textures, surface colors, reflectance coefficients, refractive indices and so on.

<sup>4</sup>Official website:<http://www.opengl.org/>

<sup>5</sup>The code of underlying reference framework is written in Java and uses JOGL and GLSL<sup>6</sup> in order to communicate with the GPU and can be found at <https://iliias.unibe.ch/>

<sup>6</sup>JOGL is a Java binding for OpenGL (official website <http://jogamp.org/jogl/www/>) and GLSL is OpenGL's high-level shading language. Further information can be found on wikipedia: [http://de.wikipedia.org/wiki/OpenGL\\_Shading\\_Language](http://de.wikipedia.org/wiki/OpenGL_Shading_Language)

lowing input data<sup>7</sup>:

- the structure of snake skin of different species<sup>8</sup> represented as discrete valued height fields acquired using AFM and stored as grayscale images.
- real measured snake geometry represented as a triangle mesh.

The first processing stage of our implementation is to compute the Fourier Terms of the provided height fields like described in section 1.4. For this preprocessing purpose we use Matlab relying on its internal, numerically fast, libraries for computing Fourier Transformations<sup>9</sup>. The next stage is to read these precomputed Fourier Terms into our Java renderer. This program also builds our manually defined rendering scene. The last processing stage of our implementation is rendering of the iridescent colorpatterns due to light diffracted on snake skins. We implemented our diffraction model from chapter 1 as OpenGL shaders. Notice that all the necessary computations in order to simulate the effect of diffraction are performed within a fragment shader. This implies that we are modeling pixelwise the effect of diffraction and hence the overall rendering quality and runtime complexity depends on rendering window's resolution.

In the following sections of this chapter we are going to explain all render processing stages in detail. First, we discuss, how our precomputation process, using Matlab, actually works. Then, we introduce our Java Framework. It is followed by the main section of this chapter, the explanation how our OpenGL shaders are implemented. The last section discusses an optimization of our fragment shader such that it will have interactive runtime.

## 2.1 Precomputations in Matlab

Our first task is to precompute the two dimensional discrete Fourier Transformations for a given input height field, representing a natural grating. For that purpose we have written a small Matlab<sup>10</sup> script conceptualized in algorithm 1. Our Matlab script reads a given image, which is representing a nano-scaled height field, and computes its two dimensional DFT (2dDFT) by using Matlab's internal Fast Fourier Transformation (FFT) function, denoted by *fft*<sup>11</sup>. Note that we only require one color channel of the input image, since the input image is representing an height field, encoded by just one color. Keep in mind that taking the Fourier transformation of an arbitrary function will result in a complex valued output which implies that we will get a complex value for frequency pairs of our input image. Therefore, for each input image we get as many output images, representing the 2dDFT, as the minimal number of taylor terms required for a well-enough approximation. In order to store our output images, we have to use two color channels instead of just one like it was for the given input image. Some example visualizations for the Fourier Transformation are shown in figure 2.1. We store these intermediate results as binary files to offer floating point precision for the run-time computations to ensure higher precision.

<sup>7</sup>All data is provided by the Laboratory of Artificial and Natural Evolution in Geneva. See their website: [www.lanevol.org](http://www.lanevol.org)

<sup>8</sup>We are using height field data for Elaphe and Xenopeltis snakes individuals like shown in figure ??

<sup>9</sup>Actually we use Matlab's inverse 2d Fast Fourier Transformation (FFT) implementation applied on different powers of quation ??. Further information can be read up in section 2.1

<sup>10</sup>Matlab is a interpreted scripting language which offers a huge collection of mathematical and numerically fast and stable algorithms.

<sup>11</sup>Remember, even we are talking about fourier transformations, in our actual computation, we have to compute the inverse fourier transformation. See paragraph ?? for further information. Furthermore our height fields are two dimensional and thus we have to compute a 2d inverse fourier transformation.

In our script every discrete frequency is normalized by its corresponding DFT extrema<sup>12</sup> in the range  $[0, 1]$  and the range extrema are stored separately for each DFT term. The normalization is computed the following way:

$$\begin{aligned} f &: [x_{min}, x_{max}] \rightarrow [0, 1] \\ x &\mapsto f(x) = \frac{x - x_{min}}{x_{max} - x_{min}} \end{aligned} \tag{2.1}$$

Where  $x_{min}$  and  $x_{max}$  denote the extreme values of a DFT term. Later, during the shading process of our implementation, we have to apply the inverse mapping. This is non-linear interpolation which is required in order to rescaled all frequency values in the DFT terms.

---

<sup>12</sup>We are talking about the i2dFFT of our height fields to the power of  $n$ . This is an  $N$  by  $N$  matrix (assuming the discrete height field was an  $N$  by  $N$  image), for which each component is a complex number. Hence, there is a complex extrema as well as a imaginary extrema.

---

**Algorithm 1** Precomputation: Pseudo code to generate Fourier terms

---

**INPUT** *heightfieldImg, maxH, dH, termCnt***OUTPUT** *DFT terms stored in Files*

```

% maxH:      A floating-point number specifying
%             the value of maximum height of the
%             height-field in MICRONS, where the
%             minimum-height is zero.
%
% dH:        A floating-point number specifying
%             the resolution (pixel-size) of the
%             'discrete' height-field in MICRONS.
%             It must be less than 0.1 MICRONS
%             to ensure proper response for
%             visible-range of light spectrum.
%
% termCnt:    An integer specifying the number of
%             Taylor series terms to use.

function ComputeFFTImages(heightfieldImg, maxH, dh, termCnt)
dh = dh*1E-6;
% load patch into heightfieldImg
patchImg = heightfieldImg.*maxH;
% rotate patchImg by 90 degrees
for t = 0 : termCnt
    patchFFT = power(1j*patchImg, t);
    fftTerm{t+1} = fftshift(fft2(patchFFT));

    % rescale terms as
    imOut(:, :, 1) = real(fftTerm{t+1});
    imOut(:, :, 2) = imag(fftTerm{t+1});
    imOut(:, :, 3) = 0.5;

    % rotate imOut by -90 degrees
    % find real and imaginary extrema of
    % write imOut, extrema, dH, into files.
end

```

---

They key idea of algorithm 1 is to compute iteratively the Fourier Transformation for different powers of the provided height field. These DFT values are scaled by according to their extrema values. Another note about the command `fftshift`: It rearranges the output of the `fft2` by moving the zero frequency component to the centre of the image. This simplifies the computation of DFT terms lookup coordinates during rendering.



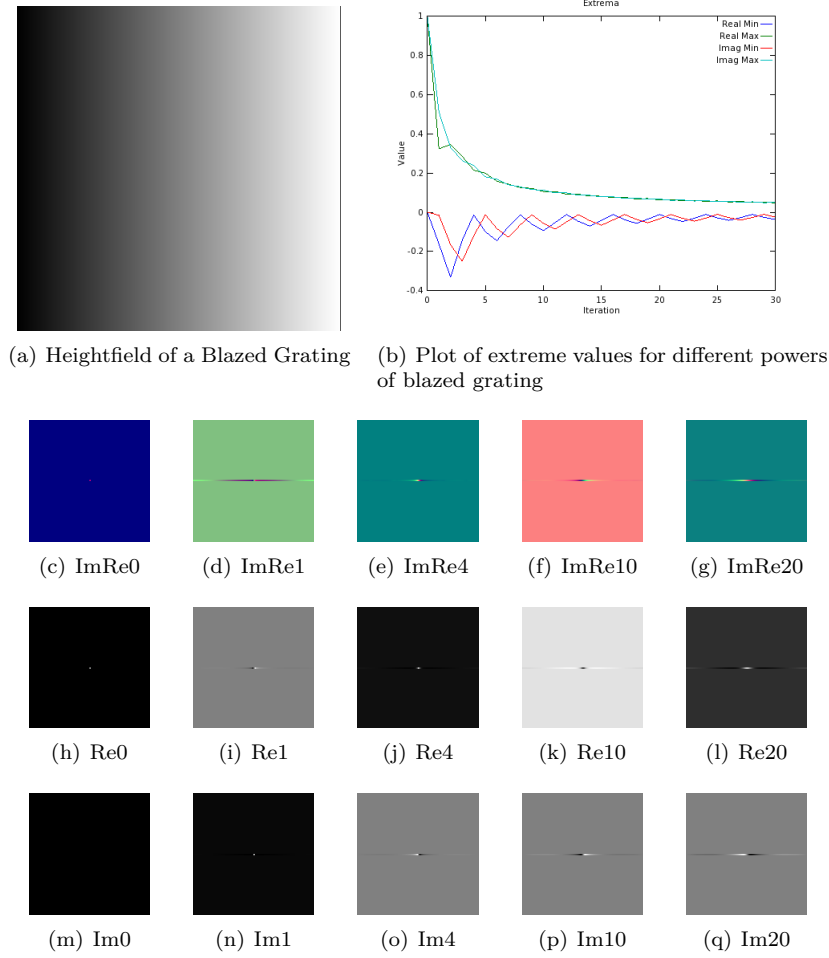


Figure 2.1: A visualization of DFT terms for a height field of a Blazed Grating.

In figure 2.1 we see examples of a visualization of Fourier Transformations generated by our Matlab script for a blazed grating<sup>13</sup> as an input height field image, shown in figure 2.1(a). Figure 2.1(b) shows plots of the extreme values of DFT terms for different powers of the blazed grating. We recognize that, the higher the power of the grating becomes, the closer the extreme values of the corresponding DFT terms get. The figure line from figure 2.1(c) until figure 2.1(g) show us example visualizations of DFT terms for different powers of our grating's height field. Remember that DFT terms are complex valued matrices of dimension as their height field has. In this visualization, all real part values are stored in the red- and the imaginary parts in the green color channel of an DFT image. The figure line from figure 2.1(h) till figure 2.1(l) show us the real part images from above's line corresponding figures. Similarly for the figure line from figure 2.1(m) until figure 2.1(q) showing the corresponding imaginary part DFT term images.

<sup>13</sup>A blazed grating is a height field consisting of ramps, periodically aligned on a given surface.

## 2.2 Java Renderer

This section explains the architecture of the rendering program which I implemented<sup>14</sup> and used for this project. The architecture of the program is divided into two parts: a rendering engine, the so called jrtr (java real time renderer) and an application program. Figure 2.2 outlines the architecture of the renderer.

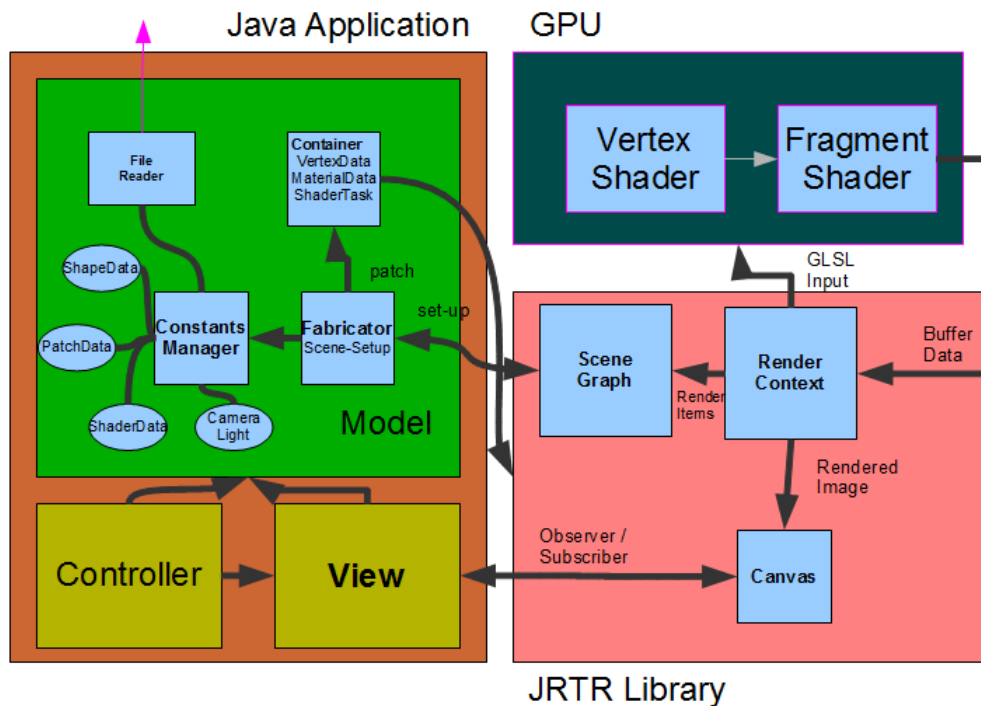


Figure 2.2: Schematic architecture of our Java renderer.

The application program relies on the MVC (Model-View-Controller) architecture pattern. The View just represents a canvas in which the rendered images are shown. The Controller implements the event listening functionalities for interactive rendering within the canvas. The Model of our application program consists of a Fabricator, a file reader and a constants manager. The main purpose of a Fabricator is to set up a rendering scene by accessing a constant manager containing many predefined scene constants. A scene consists of a camera, a light source, a frustum, shapes and their associated material constants. Such materials include a shape texture, precomputed DFT terms<sup>15</sup> for a given height field<sup>16</sup> like visualized in figure 2.1. A shape is a geometrical object defined by a triangular mesh as shown in figure 2.3.

<sup>14</sup>This program is based on the code of a java real-time renderer, developed as a student project in the computer graphics class, held by M. Zwicker in autumn 2012.

<sup>15</sup>See section 2.1 for further information.

<sup>16</sup>and other height field constants such as the maximal height of its bumps or its pixel real-world width correspondence.

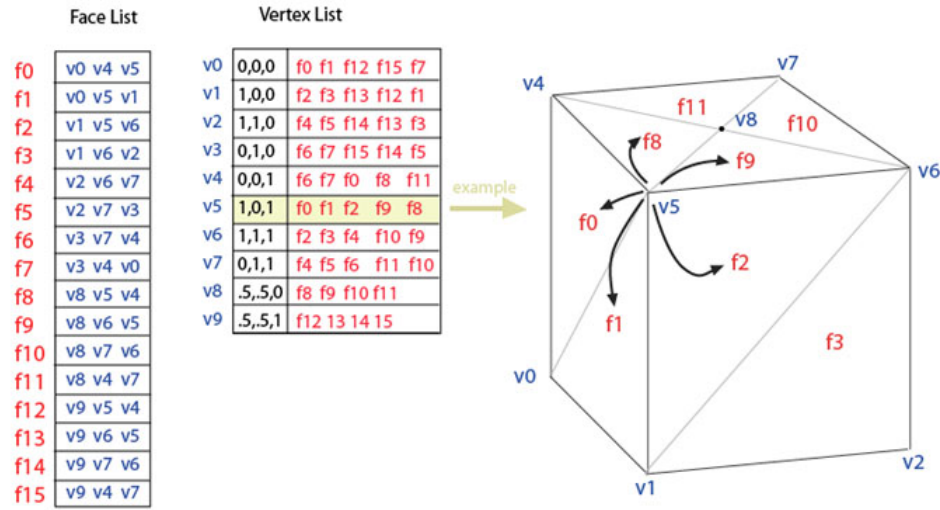


Figure 2.3: Representation<sup>17</sup> of a triangular mesh represents an object as a set of triangles and a set of vertices.

Such a mesh is represented as a data structure consisting of a list of vertices, each stored as a triplet of  $x$ ,  $y$ ,  $z$  positions and triangles, each defined by a triple of vertex-indices. Besides its position, a vertex can have further data assigned to, like a surface color, normals and texture coordinates. The whole scene is encapsulated in a scene graph data-structures, defined and managed within the rendering engine. A scene graph contains all scene geometries and their transformations in a tree like structured hierarchy.

All required configuration, in order to communicate with the GPU through OpenGL, is performed in the jrtr rendering engine. Furthermore, jrtr's render context object, the wholeresource-management for various types of low-level buffers, which are used within the rendering pipeline by our GLSL shaders, takes place in the rendering place. More precisely, this means allocating memory for the buffers, assigning them with scene data and flushing them, when not used anymore. The whole shading process is performed in the GPU, stage-wise: The first stage is the vertex shader (see section 2.3.1) followed by the fragment shader (see section 2.3.2). The jrtr framework also offers the possibility to assign user-defined shaders written in GLSL.

## 2.3 GLSL Diffraction Shader

### 2.3.1 Vertex Shader

In our implementation we want to simulate the structural colors a viewer sees when light diffracted is on grating, e.g. on the skin of a snake. For this purpose, we reproduce a 2d image of a given 3d scene as seen from the perspective of a viewer for given lightning conditions. The color computation of an image is performed in the GPU shaders of the rendering pipeline. In OpenGL, there are two basic shading stages performed to render an image whereas the vertex shader is the first shading stage in the rendering pipeline.

<sup>17</sup>Modified image which originally has been taken from [http://en.wikipedia.org/wiki/Polygon\\_mesh](http://en.wikipedia.org/wiki/Polygon_mesh)

As an input, a vertex shader receives one vertex of a mesh and other vertex data such as a vertex normals. It only can access this data and has no information about the neighborhood of a vertex or the topology of its corresponding shape. Since vertex positions of a shape are defined in a local coordinate system<sup>18</sup> and we want to render an image of the perspective of viewer, we have to transform the locally defined positions to a perspective projected viewer space. Therefore, the main purpose<sup>19</sup> of a vertex shader is to transform the position of vertices. Notice that a vertex shader can manipulate the position of a vertices, but cannot generate additional mesh vertices. Therefore, the output of any vertex shader is a transformed vertex position. Keep in mind that all vertex shader outputs will be used within the fragment shader. For an example, please have a look at our fragment shader 2.3.2.

In the following let us consider the whole transformation, applied in the vertex shader, in depth. Let  $p_{local}$  denote the position of a shape vertex, defined in a local coordinate system. Then the transformation from  $p_{local}$  into the perspective projected position as seen by a observer  $p_{projective}$  looks like the following:

$$p_{projective} = P \cdot C^{-1} \cdot M \cdot p_{local} \quad (2.2)$$

where  $P$ ,  $C^{-1}$  and  $M$  are transformation matrices<sup>20</sup>, defined the following way:

**Model matrix  $M$ :** Each vertex position of a shape is initially defined in a local coordinate system.

To make is feasible to place and transform shapes in a scene, a reference coordinate system, the so called world space, has to be introduced. Hence, for every shape a matrix  $M$  is associated, defining the transformation from its local coordinate system into the world space.

**Camera matrix  $C$ :** A camera models how the eye of a viewer sees an object, defined in world space like shown in figure 2.4. For calculating the transformation matrix  $C$ , a viewer's eye position and viewing direction, each defined in world space, are required. Therefore,  $C$  denotes a transformation from coordinates defined in camera space into the world space. Thus, in order to transform a position from world space to camera space, we have to use the inverse of  $C$ , denoted by  $C^{-1}$ .

**Frustum  $P$ :** The Matrix  $P$  defines a perspective projection onto image plance, i.e. for any given position in camera space,  $P$  determines the corresponding 2d image coordinate. Persepctive projections project along rays that converge in center of projection.

Since we are interested in modeling how a viewer sees structural colors on a given scene shape as shown in figure 2.4, modeling a viewer's eye by formulating the corresponding camera matrix  $C$ , is the most important component of the whole transformation series applied in the vertex shader. Hence, we next will have a closer look in how a camera matrix  $C$  actually can be computed.

<sup>18</sup>Defining the positions of a shape in a local coordinate system simplifies its modeling process and allows us to apply transformations to a shape.

<sup>19</sup>Furthermore, texture coordinates used for texture-lookup within the fragment shader and per vertex lightning can be computed.

<sup>20</sup>These tranformation matrices are linear transformations expressed in homogenous coordinates.

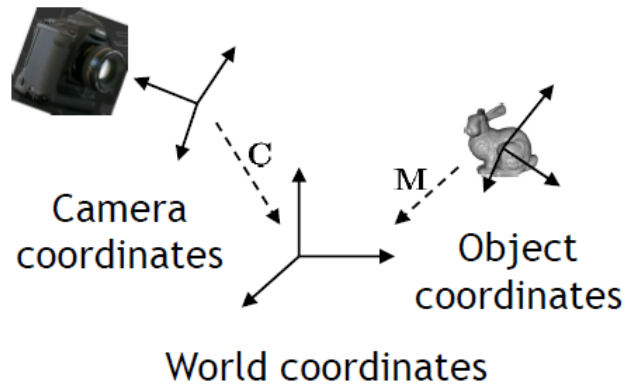


Figure 2.4: Illustration<sup>21</sup> of the Camera coordinate system where its origin defines the center of projection of camera.

The camera matrix  $C$  is constructed from its center of projection  $e$ , the position  $d$  where the camera looks at and a direction vector  $up$ , defining what is the direction in camera space pointing upwards. These components,  $e$ ,  $d$  and  $up$ , are defined in world coordinates. Figure 2.5 illustrates geometrical setup required in order to construct  $C$ .

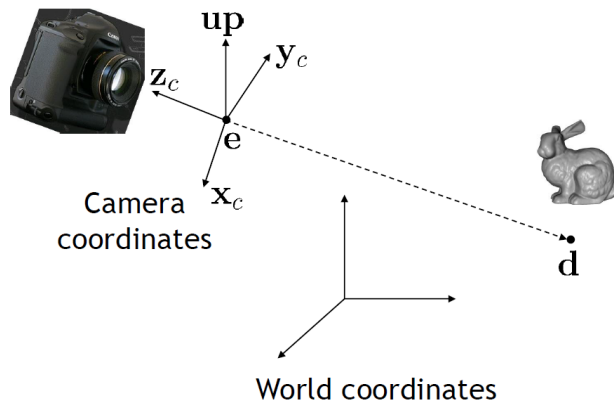


Figure 2.5: Illustration<sup>22</sup> of involved components in order to construct the camera matrix  $C$ . The eye-vector  $e$  denotes the position of the camera in space,  $d$  is the position the camera looks at, and  $up$  denotes the camera's height. The camera space is spanned by the vectors helper vectors  $x_c$ ,  $y_c$  and  $z_c$ . Notice that objects we look at are in front of us, and thus have negative  $z$  values

The mathematical representation of these vectors,  $x_c$ ,  $y_c$  and  $z_c$ , spanning the camera space, introduced in figure 2.5, looks like the following:

<sup>21</sup>This image has been taken from the lecture slides of computer graphics class 2012 which can be found on ilias.

<sup>22</sup>This image has been taken from the lecture slides of computer graphics class 2012 which can be found on ilias.

$$\begin{aligned}
z_c &= \frac{e - d}{\|e - d\|} \\
x_c &= \frac{up \times z_c}{\|up \times z_c\|} \\
y_c &= z_c \times x_c
\end{aligned} \tag{2.3}$$

As we can see,  $x_c$ ,  $y_c$  and  $z_c$  are independent unit vectors. Therefore, they span a 3d space, the so called camera matrix. In order to express a coordinate in camera space, we have to project it onto these unit vectos. Using a homogenous coordinates representation, this a projection onto these unit vectors can be formulated by the transformation matrix  $C$ :

$$C = \begin{bmatrix} x_c & y_c & z_c & e \\ 0 & 0 & 0 & 1 \end{bmatrix} \tag{2.4}$$

In our vertex shader, besides transforming the vertex positions like described in equation 2.2, for every vertex, we also compute the direction vectors  $\omega_i$  and  $\omega_r$  described like in figure ???. Those direction vectors are transformed onto the tangent space, a local coordinate system spanned by a vertex's normal, tangent and binormal vector. For further information and more insight about the the tangent space, please have a look at the appendix in the section D.3. The algorithmic idea of our vertex shader, stating all its computational steps, is conceptualized in algorithm 2.

---

**Algorithm 2** Vertex diffraction shader pseudo code

---

**Input:**     *Mesh* with vertex *normals* and *tangents*  
               Space tranformations  $\{M, C^{-1}, P\}$   
               Light direction *lightDirection*  
**Output:**   Incident light and viewer direction  $\omega_i, \omega_r$   
               Transformed position  $p_{per}$

**Procedures:** *normalize()*, *span()*, *projectVectorOnTo()*

```

1: Foreach VertexPosition position  $\in$  Mesh do
2:   vec3 N = normalize(M * vec4(normal, 0.0).xyz)
3:   vec3 T = normalize(M * vec4(tangent, 0.0).xyz)
4:   vec3 B = normalize(cross(N, T))
5:   TangentSpace = span(N, T, B)
6:   viewerDir = ((copw - position)).xyz
7:   lightDir = normalize(lightDirection)
8:    $\omega_i$  = projectVectorOnTo(lightDir, TangentSpace)
9:    $\omega_r$  = projectVectorOnTo(viewerDir, TangentSpace)
10:  normalize( $\omega_i$ ); normalize( $\omega_r$ )
11:   $p_{per}$  = P · C-1 · M · pobj
12: end for

```

---

As input, our vertex shader algorithm 2 takes a mesh with of a given scene shape. Each of this vertexc should have a normal and a tangent assigned to. Furthermore, the direction of the scene light is required. For our implementation we always used directional light sources. An example of an directional light source is given in figure 2.6.

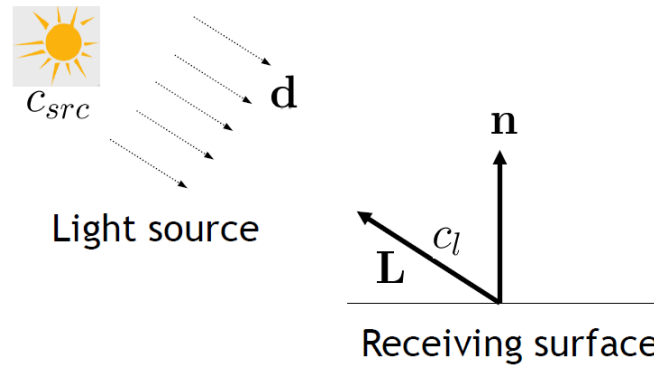


Figure 2.6: Illustration<sup>23</sup> of our light source setup. For a directional light source, all light rays are in parallel.

Last, in order to transform the positions of our mesh like described in equation 2.2, we also have to pass these transformation matrices<sup>24</sup>. For simplification purposes, we introduced the following helper procedures used in the vertex shading algorithm:

**normalize():** Computes the normalized version of a given input vector.

**span():** Assembles a matrix from a given set of vectors. This matrix spans a vector space.

**projectVectorOnTo():** Takes two arguments, a vector and a matrix. The first argument is projected onto each column of a given matrix. And returns a vector living the space spanned by the given argument matrix.

The output of our vertex shader is on the one side the transformed vertex position and on the other side the incident light  $\omega_i$  and viewing direction  $\omega_r$  both transformed into the tangent space. The output of the vertex shader is used as the input of the fragment shader, discussed in the next section.

### 2.3.2 Fragment Shader

In the previous section we gave an introduction to the first shading stage of the OpenGL rendering pipeline by explaining the basics of a vertex shaders. Furthermore, we conceptually discussed the idea behind our vertex shading algorithm formulated in algorithm 2. Summarized, the main purpose of our vertex shader is to compute the light- and viewing-direction vectors  $\omega_i$  and  $\omega_r$  defined like in figure ??.

After the vertex-shading stage, the next stage in the OpenGL rendering pipeline is the *rasterization* of mesh triangles. As an input, a rasterizer takes a triple of mesh-triangle spanning vertices, each previously processed by a vertex shader. For each pixel lying inside the current mesh triangle, a rasterizer computes its corresponding position in the triangle. According to its computed position, a pixel also gets interpolated values of the vertices attributes of its mesh triangle assigned. The set of interpolated vertex attributes together with the computed position of a pixel is denoted as a fragment. Figure 2.7 conceptualizes the idea of processed set of fragment computed by a rasterizer.

<sup>23</sup>This image has been taken from the lecture slides of computer graphics class 2012 which can be found on ilias.

<sup>24</sup>When speaking about transformation matrices, we are referring to the model, camera and frustum matrix.

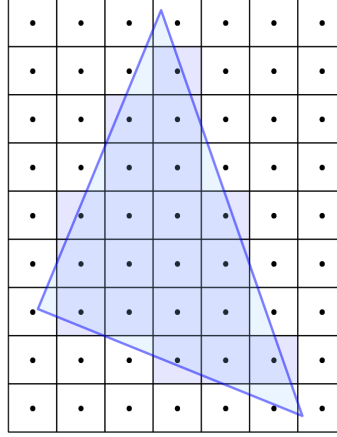


Figure 2.7: Illustration<sup>25</sup> of fragments covered by mesh triangle computed by the OpenGL rasterizer.

A fragment shader as shown in figure *FIGUREFRSGEMNTSHADER*, is the OpenGL pipeline stage subsequent after a mesh triangle is rasterized in the rasterization stage. As input value, a fragment shader takes at least a fragment computed by the rasterizer. It is also possible to assign custom, non-interpolated values to a fragment shader. For each fragment in the fragment shading stage, a color value is computed. Furthermore, a fragment shader computes a depth value for each of its fragments, determining their visibility. Since all existing scene vertices were perspectively projected onto the 2d image plane, the rasterizer could have produced several fragments having assigned the same pixel position. Therefore, among all fragments with the same pixel position, the outputted pixel color is equal to the color of that fragment, which depth is closest to the viewer.

In this section we explain how to render structural colors resulting due to light diffracted on a natural grating, based on the model described in section 1.5. The color values of the produced structural colors, resulting from our model, are computed by our fragment shader which expects being provided by the following input:

- Precompute DFT terms of the provided height field as explain in section 2.1.
- The processed output, produced during the vertex shading stage (see section 2.3.1), which is, the light- and viewing-direction vectors  $\omega_i$  and  $\omega_r$ .
- Fragments produced during the rasterization stage using the output of our vertex shader.

Apart from these basic, varying input values, the following set of shading constants are initialized:

- The number of iterations used for the Taylor series approximation, determining the approximation accuracy.
- The wavelength spectrum  $\Lambda = [\lambda_{min}, \lambda_{max}]$  with a certain discretizing level  $\lambda_{step}$ .

<sup>25</sup>This image was taken from [http://en.wikibooks.org/wiki/GLSL\\_Programming/Rasterization](http://en.wikibooks.org/wiki/GLSL_Programming/Rasterization)



- The color weights of the  $CIE_{XYZ}$  color matching functions.
- The height field image resolution and its pixel to width correspondance.

Using all these inputs, our fragment shader performs a numerical integration over the given wavelength spectrum  $\Lambda$  for our final derived expression, stated in equation 1.33. For this integration we use the trapezoidal-rule with uniform discretization of the wavelength spectrum at  $\lambda_{step} = 5nm$  step sizes. This implies we are compressing sampled frequencies to the region near the origin due to the fact we are dividing the  $(u, v)$  by the wavelength  $\lambda$  and this implies that the  $(u, v)$  space is sampled non-linearly.

In section 1.2.3 we have seen that we have to multiply our DFT terms by a Gaussian Window in order to approximate the DTFT which our model is based on. This windowing approach is performed for each discrete  $\lambda$  value using a window large enough to span  $4\sigma_f$  in both dimensions. Our DFT terms are computed from height fields that span at least  $65\mu m^2$  and are sampled at a resolution of at least  $100\mu m$ . This ensures that the spectral response encompasses all the wavelengths in the visible spectrum.

Next, we will discuss the actual fragment shading algorithm, listed in algorithm 3. But before doing so, let us first introduce some helper procedures which are used by our fragment shading algorithm.

**Algorithm 3** Fragment diffraction shader pseudo code

---

**Input:** Precomputed DFT Terms  
Mesh Triangles  
 $\omega_i$  and  $\omega_r$

**Output:** Structural Color of a pixel

**Procedures**<sup>26</sup>: *getColorWeights*: get colormatching value for wavelength  $\lambda$   
*getlookupCoords*: get lookup coordinate of given viewing- and light direction  
*distVecFromOriginTo*: get direction vector from origin to a given position  
*getLocalLookUp*: computes lookup coordinate to dertermine DFT value for windwowing.  
*rescaledFourierValueAt*: rescales dft terms according to equation 2.1  
*gaussWeightOf*: computes gaussian window according to equation 1.8  
*dot*: computes the dot-product of two given vectors  
*gammaCorrect*: apply camma correction on rgb vector

---

```

1: Foreach Pixel  $p \in$  Fragment do
2:   INIT  $BRDF_{XYZ}, BRDF_{RGB}$  TO  $vec4(0.0)$ 
3:    $(u, v, w) = -\omega_i - \omega_r$ 
4:   for  $(\lambda = \lambda_{min}; \lambda \leq \lambda_{max}; \lambda = \lambda + \lambda_{step})$  do
5:      $xyzWeights = getColorWeights(\lambda)$ 
6:      $lookupCoord = getlookupCoords(u, v, \lambda)$ 
7:     INIT  $P$  TO  $vec2(0.0)$ 
8:      $k = \frac{2\pi}{\lambda}$ 
9:     for  $(n = 0$  TO  $T)$  do
10:       $taylorScaleF = \frac{(kw)^n}{n!}$ 
11:      INIT  $F_{fft}$  TO  $vec2(0.0)$ 
12:       $anchorX = int(floor(center.x + lookupCoord.x * fftImWidth))$ 
13:       $anchorY = int(floor(center.y + lookupCoord.y * fftImHeight))$ 
14:      for  $(i = (anchorX - winW)$  TO  $(anchorX + winW))$  do
15:        for  $(j = (anchorY - winW)$  TO  $(anchorY + winW))$  do
16:           $dist = distVecFromOriginTo(i, j)$ 
17:           $pos = getLocalLookUp(i, j, n)$ 
18:           $fftVal = rescaledFourierValueAt(pos)$ 
19:           $fftVal *= gaussWeightOf(dist)$ 
20:           $F_{fft} += fftVal$ 
21:        end for
22:      end for
23:       $P += taylorScaleF * F_{fft}$ 
24:    end for
25:     $xyzPixelColor += dot(vec3(|P|^2), xyzWeights)$ 
26:  end for
27:   $BRDF_{XYZ} = xyzPixelColor * C(\omega_i, \omega_r) * shadowF$ 
28:   $BRDF_{RGB}.xyz = D_{65} * M_{XYZ-RGB} * BRDF_{XYZ}.xyz$ 
29:   $BRDF_{RGB} = gammaCorrect(BRDF_{RGB})$ 
30: end for

```

---

<sup>26</sup>Please have a look at section 2.3.2 to see a description of these procedures in detail

Please note that for simplification purposes we omitted some input values in algorithm 3. A complete input value list can be found in section 2.3.2. Last, a brief description of some code sections of our fragment shading algorithm:

**From line 4 to 26:**

This loop performs uniform sampling along wavelength-space. *ColorWeights*( $\lambda$ ) computes the color weight for the current wavelength  $\lambda$  by linear interpolation between the color weight for  $\lceil \lambda \rceil$  and  $\lfloor \lambda \rfloor$  which are stored in an external weights-table (assuming this table contains wavelengths in 1nm steps). At line 6: *lookupCoord*( $u, v, \lambda$ ) the coordinates for the texture lookup are computed - See 2.7. Line 25 sums up the diffraction color contribution for the current wavelength in iteration  $\lambda$ .

**From line 9 to 24:**

This loop performs the Taylor series approximation using T terms. Basically, the spectral response is approximated for our current ( $u, v, \lambda$ ). Furthermore, neighborhood boundaries for the gaussian-window sampling are computed, denoted as anchorX and anchorY.

**From line 14 to 22:**

In this inner most loop, the convolution of the gaussian window with the DFT of the patch is performed. *gaussWeightOf*(*dist*) computes the weights in equation (1.8) from the distance between the current pixel's coordinates and the current neighbor's position in texture space. Local lookup coordinates for the current fourier coefficient *fftVal* value are computed at line 17 and computed like described in 2.9. The actual texture lookup is performed at line 18 using those local coordinates. Inside *rescaledFourierValueAt* the values *fftVal* is rescaled by its extrema, i.e. (*fftVal* \* *Max* + *Min*) is computed, since *fftVal* is normalized 2.1. The current *fftVal* values in iteration is scaled by the current gaussian weight and then summed to the final neighborhood FFT contribution at line 20.

**After line 26:**

At line 27 the gain factor  $C(\omega_i, \omega_r)$  1.18 is multiplied by the current computed pixel color like formulated in 1.19. The gain factor contains the geometric term *refeq*: *geometricterm* and the Fresnel term *F*. We approximate *F* by the Schlick approximation D.1, using a refractive index at 1.5 since this is close to the measured value from snake sheds. Our BRDF values are scaled by a shadowing function as described in (SEE REFERENCES - PAPER), since most of the grooves in the snake skin nano-structures would form a V-cavity along the plane for a wave front with their top-edges at almost the same height. Last, we transform our colors from the  $CIE_{XYZ}$  colorspace to the  $CIE_{RGB}$  space using the CIE Standard Illuminant D65, followed by a gamma correction. See 2.4.3 for further insight.

## 2.4 Technical details

### 2.4.1 Texture lookup

In a GLSL shader the texture coordinates are normalized which means that the size of the texture maps to the coordinates on the range  $[0, 1]$  in each dimension. By convention the bottom left corner of an image has the coordinates (0,0), whereas the top right corner has the value (1,1) assigned.

Given a nano-scaled surface patch  $P$  with a resolution  $A$  by  $A$  microns stored as an  $N$  by  $N$  pixel image  $I$ . Then one pixel in any direction corresponds to  $dH = \frac{A}{N} \mu m$ . In Matlab we compute a series of  $n$  output images  $\{I_{out_1}, \dots, I_{out_n}\}$  from  $I$ , which we will use for the lookup in our shader - See figure 2.8. For the lookup we use scaled and shifted  $(u, v)$  coordinates from ??.

Since the zero frequency component of output images was shifted towards the centre of each image, we have to shift  $u, v$  to the center of the current  $N$  by  $N$  pixel image by a bias  $b$ . Mathematically, the bias is a constant value is computed the following:

$$b = (N \% 2 == 0) \quad ? \quad \frac{N}{2} : \frac{N-1}{2} \quad (2.5)$$

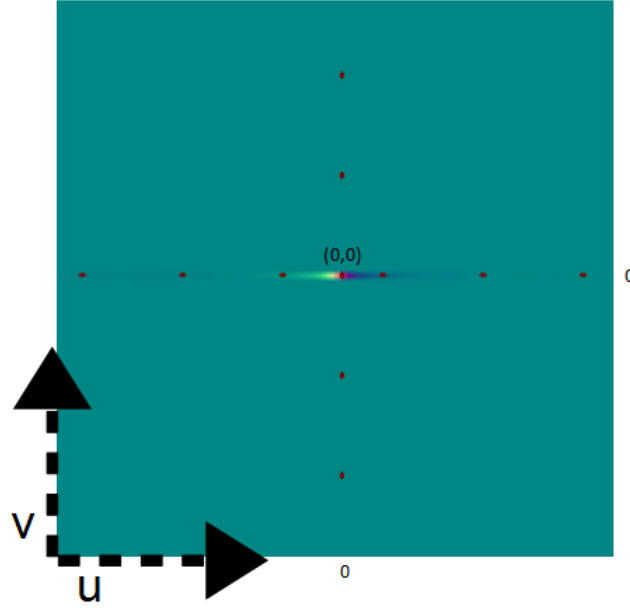


Figure 2.8:  $(u, v)$  lookup image

For the scaling we have to think a little further: let's consider a  $T$  periodic signal in time, i.e.  $x(t) = x(t + nT)$  for any integer  $n$ . After applying the DFT, we have its discrete spectrum  $X[n]$  with frequency interval  $w_0 = 2\pi/T$  and time interval  $t_0$ . Let  $k = \frac{2\pi}{\lambda}$  denote the wavenumber for the current wavelength  $\lambda$ . Then the signal is both periodic with time period  $T$  and discrete with time interval  $t_0$  then its spectrum should be both discrete with frequency interval  $w_0$  and periodic with frequency period  $\Omega = \frac{2\pi}{t_0}$ . This gives us the idea how to discretize the spectrum: Let us consider our Patch  $P$  assuming it is distributed as a periodic function on our surface. Then, its frequency interval along the  $x$  direction is  $w_0 = \frac{2\pi}{T} = \frac{2\pi}{N \cdot dH}$ . Thus only wave numbers that are integer multiples of  $w_0$  after a multiplication with  $u$  must be considered, i.e.  $ku$  is integer multiple of  $w_0$ . Hence the lookup for the  $u$ -direction will look like:

$$\frac{ku}{w_0} = \frac{kuNdH}{2\pi} \quad (2.6)$$

$$= \frac{uNdH}{\lambda} \quad (2.7)$$

Using those findings 2.5, 2.7, the final  $(u, v)$  texture lookup-coorinates for the current wavelength  $\lambda$  in iteration, will then look like:

$$(u_{lookup}, v_{lookup}) = \left( \frac{uNdH}{\lambda} + b, \frac{vNdH}{\lambda} + b \right) \quad (2.8)$$

Note for the windowing approach we are visiting a one pixel neighborhood for each pixel  $p$ . This is like a base change with  $(u_{lookup}, v_{lookup})$  as new coordinate system origin. The lookup coordinates for the neighbor-pixel  $(i, j)$  are:

$$(u_{lookup}, v_{lookup}) = (i, j) - (u_{lookup}, v_{lookup}) \quad (2.9)$$

### 2.4.2 Texture Blending

The final rendered color for each pixel is a weighted average of different color components, such as the diffraction color, the texture color and the diffuse color. In our shader the diffraction color is weighted by a constant  $w_{diffuse}$ . the texture color is once scales by a binary weight determined by the absolute value of the Fresnel Term  $F$  and once by  $1 - w_{diffuse}$ .

---

#### Algorithm 4 Texture Blending

---

```

 $\alpha = (abs(F) > 1)?1:0$ 
 $c_{out} = (1 - w_{diffuse}) * c_{diffraction} + (1 - \alpha) * c_{texture} + w_{diffuse} * c_{texture}$ 

```

---

### 2.4.3 Color Transformation

In our shader we access a table which contains precomputed CIE's color matching functions values from  $\lambda_{min} = 380nm$  to  $\lambda_{max} = 780nm$  in  $5nm$  steps. Such a function value table can be found at downloaded at [cvrl.ioo.ucl.ac.uk](http://cvrl.ioo.ucl.ac.uk) for example. We compute the  $(X, Y, Z)$   $CIE_{XYZ}$  color values as described in section ??.

We can transform the color values into  $CIE_{RGB}$  by performing the following linear transformation:

$$\begin{bmatrix} R \\ G \\ B \end{bmatrix} = M \cdot \begin{bmatrix} X \\ Y \\ Z \end{bmatrix} \quad (2.10)$$

where one possible transformation is:

$$M = \begin{bmatrix} 0.41847 & -0.15866 & -0.082835 \\ -0.091169 & 0.25243 & 0.015708 \\ 0.00092090 & -0.0025498 & 0.17860 \end{bmatrix} \quad (2.11)$$

There are some other color space transformation. The shader uses the CIE Standard Illuminant D65 which is intended to represent average daylight. Using D65 the whole colorspace transformation will look like:

$$\begin{bmatrix} R \\ G \\ B \end{bmatrix} = M \cdot \begin{bmatrix} X \cdot D65.x \\ Y \cdot D65.y \\ Z \cdot D65.z \end{bmatrix} \quad (2.12)$$

Last we perfrom gamma correction on each pixel's  $(R, G, B)$  value. Gamma correction is a non linear transformation which controls the overall brightness of an image.

## 2.5 Discussion

The fragment shader algorithm described in 3 performs the gaussian window approach by sampling over the whole wavelength spectrum in uniform step sizes. This algorithm is valid but also slow since we iterate for each pixel over the whole lambda spectrum. Furthermore, for any pixel, we iterate over its 1 neighborhood. Considering the loop for the taylor approximation as well, we will have a run-time complexity of  $O(\#spectrumIter \cdot \#taylorIter \cdot neighborhoodRadius^2)$ . Hence, Instead sampling over the whole wavelength spectrum, we could instead integrate over just a few required lambdas which are elicited like the following: Lets consider  $(u, v, w)$  defined as ???. Let  $d$  be the spacing between two slits of a grating. For any  $L(\lambda) \neq 0$  it follows  $\lambda_n^u = \frac{du}{n}$  and  $\lambda_n^v = \frac{dv}{n}$ . For  $n = 0$  there it follows  $(u, v) = (0, 0)$ . If  $u, v > 0$

$$N_{min}^u = \frac{du}{\lambda_{max}} \leq n_u \leq \frac{du}{\lambda_{min}} = N_{min}^u$$

$$N_{min}^v = \frac{dv}{\lambda_{max}} \leq n_v \leq \frac{dv}{\lambda_{min}} = N_{min}^v$$

If  $u, v < 0$

$$N_{min}^u = \frac{du}{\lambda_{min}} \leq n_u \leq \frac{du}{\lambda_{min}} = N_{max}^u$$

$$N_{min}^v = \frac{dv}{\lambda_{min}} \leq n_v \leq \frac{dv}{\lambda_{min}} = N_{max}^v$$

By transforming those equation to  $(\lambda_{min}^u, \lambda_{min}^u)$ ,  $(\lambda_{min}^v, \lambda_{min}^v)$  respectively for any  $(u, v, w)$  for each pixel we can reduce the total number of required iterations in our shader.

Another variant is the PQ approach described in chapter 2 1.6.1. Depending on the interpolation method, there are two possible variants we can think of as described in 1.6.2. Either we try to interpolate linearly or use sinc interpolation. The first variant does not require to iterate over a pixel's neighborhood, it is also faster than the gaussian window approach. One could think of a combination of those two optimization approaches. Keep in mind, both of these approaches are further approximation. The quality of the rendered images will suffer using those two approaches. The second variant, using the sinc function interpolation is well understood in the field of signal processing and will give us reliable results. The drawback of this approach is that we again have to iterate over a neighborhood within the fragment shader which will slow down the whole shading. The following algorithm describes the modification of the fragment shader 3 in order to use sinc interpolation for the PQ approach 1.6.1.

---

**Algorithm 5** Sinc interpolation for PQ approach

---

**Foreach** Pixel  $p \in Image I$  **do**

$$w_p = \sum_{(i,j) \in \mathcal{N}_1(p)} sinc(\Delta_{p,(i,j)} \cdot \pi + \epsilon) \cdot I(i, j)$$

$$c_p = w_p \cdot (p^2 + q^2)^{\frac{1}{2}}$$

$$render(c_p)$$

**end for**

---

In a fragment shader we compute for each pixel  $p$  in the current fragment its reconstructed function value  $f(p)$  stores in  $w_p$ .  $w_p$  is the reconstructed signal value at  $f(p)$  by the sinc function as described in 1.6.2. We calculate the distance  $\Delta_{p,(i,j)}$  between the current pixel  $p$  and each of its neighbor pixels  $(i, j) \in \mathcal{N}_1(p)$  in its one-neighborhood. Multiplying this distance by  $\pi$  gives us

---

the an angle used for the sinc function interpolation. We add a small integer  $\epsilon$  in order to avoid division by zeros side-effects.

# Appendix A

## Signal Processing Basics

A signal is a function that conveys information about the behavior or attributes of some phenomenon. In the physical world, any quantity exhibiting variation in time or variation in space (such as an image) is potentially a signal that might provide information on the status of a physical system, or convey a message between observers.

The Fourier Transform is an important image processing tool which is used to decompose an image into its sine and cosine components. The output of the transformation represents the image in the Fourier or frequency domain, while the input image is the spatial domain equivalent. In the Fourier domain image, each point represents a particular frequency contained in the spatial domain image.

### A.1 Fourier Transformation

The Fourier-Transform is a mathematical tool which allows to transform a given function or rather a given signal from defined over a time- (or spatial-) domain into its corresponding frequency-domain.

Let  $f$  an measurable function over  $\mathbb{R}^n$ . Then, the continuous Fourier Transformation(**FT**), denoted as  $\mathcal{F}\{f\}$  of  $f$ , ignoring all constant factors in the formula, is defined as:

$$\mathcal{F}_{FT}\{f\}(w) = \int_{\mathbb{R}^n} f(x)e^{-iwt}dt \quad (\text{A.1})$$

whereas its inverse transform is defined like the following which allows us to obtain back the original signal:

$$\mathcal{F}_{FT}^{-1}\{f\}(w) = \int_{\mathbb{R}} \mathcal{F}\{w\}e^{iwt}dt \quad (\text{A.2})$$

Usual  $w$  is identified by the angular frequency which is equal  $w = \frac{2\pi}{T} = 2\pi v_f$ . In this connection,  $T$  is the period of the resulting spectrum and  $v_f$  is its corresponding frequency.

By using Fourier Analysis, which is the approach to approximate any function by sums of simpler trigonometric functions, we gain the so called Discrete Time Fourier Transform (in short **DTFT**). The DTFT operates on a discrete function. Usually, such an input function is often created by digitally sampling a continuous function. The DTFT itself is operation on a discretized signal on a continuous, periodic frequency domain and looks like the following:



$$\mathcal{F}_{DTFT}\{f\}(w) = \sum_{-\infty}^{\infty} f(x)e^{-iwx} \quad (\text{A.3})$$

Note that the DTFT is not practically suitable for digital signal processing since there a signal can be measured only in a finite number of points. Thus, we can further discretize the frequency domain and will get then the Discrete Fourier Transformation (in short **DFT**) of the input signal:

$$\mathcal{F}_{DFT}\{f\}(w) = \sum_{n=0}^{N-1} f(x)e^{-iwn} \quad (\text{A.4})$$

Where the angular frequency  $w_n$  is defined like the following  $w_n = \frac{2\pi n}{N}$  and  $N$  is the number of samples within an equidistant period sampling.

Any continuous function  $f(t)$  can be expressed as a series of sines and cosines. This representation is called the Fourier Series (denoted by FS) of  $f(t)$ .

$$f(t) = \frac{1}{2}a_0 + \sum_{n=1}^{\infty} a_n \cos(nt) + \sum_{n=1}^{\infty} b_n \sin(nt) \quad (\text{A.5})$$

where

$$\begin{aligned} a_0 &= \int_{-\pi}^{\pi} f(t)dt \\ a_n &= \frac{1}{\pi} \int_{-\pi}^{\pi} f(t)\cos(nt)dt \\ b_n &= \frac{1}{\pi} \int_{-\pi}^{\pi} f(t)\sin(nt)dt \end{aligned} \quad (\text{A.6})$$

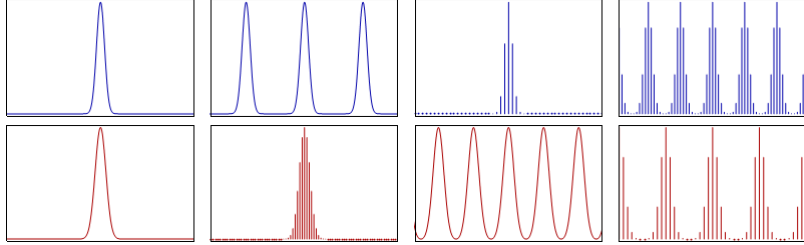


Figure A.1: Relationship<sup>1</sup> between the continuous Fourier transform and the discrete Fourier transform: Left column: A continuous function (top) and its Fourier transform A.1 (bottom). Center-left column: Periodic summation of the original function (top). Fourier transform (bottom) is zero except at discrete points. The inverse transform is a sum of sinusoids called Fourier series A.5. Center-right column: Original function is discretized (multiplied by a Dirac comb) (top). Its Fourier transform (bottom) is a periodic summation (DTFT) of the original transform. Right column: The DFT A.4 (bottom) computes discrete samples of the continuous DTFT A.3. The inverse DFT (top) is a periodic summation of the original samples.

<sup>1</sup>image of illustration has been taken from wikipedia

Spetail signal $f(t)$ is	Operator	Transformed frequency signal $\hat{f}(\omega)$ is
continuous and periodic in $t$	FS A.5	only discrete in $\omega$
only continuous in $t$	FT A.1	only continuous in $\omega$
only discrete in $t$	DTFT A.3	continuous and periodic in $\omega$
discrete and periodic in $t$	DFT A.4	discrete and periodic in $\omega$

Table A.1: Fourier operator to apply for a given spatial input signal and the properties of its resulting output signal in frequency space

## A.2 Convolution

The convolution  $f * g$  of two functions  $f, g: \mathbb{R}^n \rightarrow \mathbb{C}$  is defined as:

$$(f * g)(t) = \int_{\mathbb{R}^n} f(t)g(t - x)dx \quad (\text{A.7})$$

Note that the Fourier transform of the convolution of two functions is the product of their Fourier transforms. This is equivalent to the fact that Convolution in spatial domain is equivalent to multiplication in frequency domain. Therefore, the inverse Fourier transform of the product of two Fourier transforms is the convolution of the two inverse Fourier transforms. Last an illustration of the relationships between the previous presented Fourier transformations and different given input signals. First an concrete example shown in Figure A.1. Table A.1 tells what Fourier transformation operator has to be applied to which kind of input signal and what properties its resulting Fourier transform will have.

## A.3 Taylor Series

Taylor series is a representation of a function as an infinite sum of terms that are calculated from the values of the function's derivatives at a single point.

The Taylor series  $\mathcal{T}$  of a real or complex-valued function  $f(x)$  that is infinitely differentiable at a real or complex number  $a$  is the power series:

$$\mathcal{T}(f; a)(x) = \sum_{n=0}^{\infty} \frac{f^n(a)}{n!} (x - a)^n \quad (\text{A.8})$$

## Appendix B

# Summary of Stam's Derivations

In his paper about Diffraction Shader, J. Stam derives a BRDF which is modeling the effect of diffraction for various analytical anisotropic reflexion models relying on the so called scalar wave theory of diffraction for which a wave is assumed to be a complex valued scalar. It's noteworthy, that Stam's BRDF formulation does not take into account the polarization of the light. Fortunately, light sources like sunlight and light bulbs are unpolarized.

A further assumption in Stam's Paper is, the emanated waves from the source are stationary, which implies the wave is a superposition of independent monochromatic waves. This implies that each wave is associated to a definite wavelength  $\lambda$ . However, sunlight once again fulfills this fact.

In our simulations we will always assume we have given a directional light source, i.e. sunlight. Hence, Stam's model can be used for our derivations.

For his derivations Stam uses the Kirchhoff integral<sup>1</sup>, which is relating the reflected field to the incoming field. This equation is a formalization of Huygen's well-known principle that states that if one knows the wavefront at a given moment, the wave at a later time can be deduced by considering each point on the first wave as the source of a new disturbance. Mathematically speaking, once the field  $\psi_1 = e^{ik\mathbf{x}\cdot\mathbf{s}}$  on the surface is known, the field  $\psi_2$  everywhere else away from the surface can be computed. More precisely, we want to compute the wave  $\psi_2$  equal to the reflection of an incoming planar monochromatic wave  $\psi_1 = e^{ik\omega_i\cdot\mathbf{x}}$  traveling in the direction  $\omega_i$  from a surface  $S$  to the light source. Formally, this can be written as:

$$\psi_2(\omega_i, \omega_r) = \frac{ike^{iKR}}{4\pi R} (F(-\omega_i - \omega_r) - (-\omega_i + \omega_r)) \cdot I_1(\omega_i, \omega_r) \quad (\text{B.1})$$

with

$$I_1(\omega_i, \omega_r) = \int_S \hat{\mathbf{n}} e^{ik(-\omega_i - \omega_r)\cdot\mathbf{s}} d\mathbf{s} \quad (\text{B.2})$$

In applied optics, when dealing with scattered waves, one does use differential scattering cross-section rather than defining a BRDF which has the following identity:

$$\sigma^0 = 4\pi \lim_{R \rightarrow \infty} R^2 \frac{\langle |\psi_2|^2 \rangle}{\langle |\psi_1|^2 \rangle} \quad (\text{B.3})$$

where  $R$  is the distance from the center of the patch to the receiving point  $x_p$ ,  $\hat{\mathbf{n}}$  is the normal of the surface at  $\mathbf{s}$  and the vectors:

---

<sup>1</sup>See [http://en.wikipedia.org/wiki/Kirchhoff\\_integral\\_theorem](http://en.wikipedia.org/wiki/Kirchhoff_integral_theorem) for further information.

The relationship between the BRDF and the scattering cross section can be shown to be equal to

$$BRDF = \frac{1}{4\pi} \frac{1}{A} \frac{\sigma^0}{\cos(\theta_i)\cos(\theta_r)} \quad (B.4)$$

where  $\theta_i$  and  $\theta_r$  are the angles of incident and reflected directions on the surface with the surface normal  $n$ . See ??.

The components of vector resulting by the difference between these direction vectors: In order to simplify the calculations involved in his vectorized integral equations, Stam considers the components of vector

$$(u, v, w) = -\omega_i - \omega_r \quad (B.5)$$

explicitly and introduces the equation:

$$I(ku, kv) = \int_S \hat{\mathbf{n}} e^{ik(u,v,w) \cdot \mathbf{s}} d\mathbf{s} \quad (B.6)$$

which is a first simplification of B.2. Note that the scalar  $w$  is the third component of ?? and can be written as  $w = -(\cos(\theta_i) + \cos(\theta_r))$  using spherical coordinates. The scalar  $k = \frac{2\pi}{\lambda}$  represent the wavenumber.

During his derivations, Stam provides a analytical representation for the Kirchhoff integral assuming that each surface point  $s(x, y)$  can be parameterized by  $(x, y, h(x, y))$  where  $h$  is the height at the position  $(x, y)$  on the given  $(x, y)$  surface plane. Using the tangent plane approximation for the parameterized surface and plugging it into B.6 he will end up with:

$$\mathbf{I}(ku, kv) = \int \int (-h_x(x, y), -h_y(x, y), 1) e^{ikwh(x, y)} e^{ik(ux+vy)} dx dy \quad (B.7)$$

For further simplification Stam formulates auxillary function which depends on the provided height field:

$$p(x, y) = e^{ikwh(x, y)} \quad (B.8)$$

which will allow him to further simplify his equation B.7 to:

$$\mathbf{I}(ku, kv) = \int \int \frac{1}{ikw} (-p_x, -p_y, ikwp) dx dy \quad (B.9)$$

where he used that  $(-h_x(x, y), -h_y(x, y), 1) e^{ikwh(x, y)}$  is equal to  $\frac{(-p_x, -p_y, ikwp)}{ikw}$  using the definition of the partial derivatives applied to the function ??.

Let  $P(x, y)$  denote the Fourier Transform (FT) of  $p(x, y)$ . Then, the differentiation with respect to  $x$  respectively to  $y$  in the Fourier domain is equivalent to a multiplication of the Fourier transform by  $-iku$  or  $-ikv$  respectively. This leads him to the following simplification for B.7:

$$\mathbf{I}(ku, kv) = \frac{1}{w} P(ku, kv) \cdot (u, v, w) \quad (B.10)$$

Let us consider the term  $g = (F(-\omega_i - \omega_r) - (-\omega_i + \omega_r))$ , which is a scalar factor of B.1. The dot product with  $g$  and  $(-\omega_i - \omega_r)$  is equal  $2F(1 + \omega_i \cdot \omega_r)$ . Putting this finding and the identity B.10 into B.1 he will end up with:

$$\psi_2(\omega_i, \omega_r) = \frac{ike^{iKR}}{4\pi R} \frac{2F(1 + \omega_i \cdot \omega_r)}{w} P(ku, kv) \quad (B.11)$$

By using the identity *B.4*, this will lead us to his main finding:

$$BRDF_\lambda(\omega_i, \omega_r) = \frac{k^2 F^2 G}{4\pi^2 A w^2} \langle |P(ku, kv)|^2 \rangle \quad (\text{B.12})$$

where  $G$  is the so called geometry term which is equal:

$$G = \frac{(1 + \omega_i \cdot \omega_r)^2}{\cos(\theta_i) \cos(\theta_r)} \quad (\text{B.13})$$

# Appendix C

## Derivation Steps in Detail

### C.1 Taylor Series Approximation

For an  $N \in \mathbb{N}$  such that

$$\sum_{n=0}^N \frac{(ikwh)^n}{n!} \mathcal{F}\{h^n\}(\alpha, \beta) \approx P(\alpha, \beta) \quad (\text{C.1})$$

we have to prove:

1. Show that there exist such an  $N \in \mathbb{N}$  s.t the approximation holds true.
2. Find a value for  $B$  s.t. this approximation is below a certain error bound, for example machine precision  $\epsilon$ .

#### C.1.1 Proof Sketch of 1.

By the **ratio test** (see [1]) It is possible to show that the series  $\sum_{n=0}^N \frac{(ikwh)^n}{n!} \mathcal{F}\{h^n\}(\alpha, \beta)$  converges absolutely:

**Proof:** Consider  $\sum_{k=0}^{\infty} \frac{y^k}{k!}$  where  $a_k = \frac{y^k}{k!}$ . By applying the definition of the ratio test for this series it follows:

$$\forall y : \limsup_{k \rightarrow \infty} \left| \frac{a_{k+1}}{a_k} \right| = \limsup_{k \rightarrow \infty} \frac{y}{k+1} = 0 \quad (\text{C.2})$$

Thus this series converges absolutely, no matter what value we will pick for  $y$ .

#### C.1.2 Part 2: Find such an $N$

Let  $f(x) = e^x$ . We can formulate its Taylor-Series, stated above. Let  $P_n(x)$  denote the  $n$ -th Taylor polynomial,

$$P_n(x) = \sum_{k=0}^n \frac{f^{(k)}(a)}{k!} (x-a)^k \quad (\text{C.3})$$

where  $a$  is our developing point (here  $a$  is equal zero).

We can define the error of the  $n$ -th Taylor polynomial to be  $E_n(x) = f(x) - P_n(x)$ . the error of the  $n$ -th Taylor polynomial is difference between the value of the function and the Taylor polynomial. This directly implies  $|E_n(x)| = |f(x) - P_n(x)|$ . By using the Lagrangian Error Bound it follows:

$$|E_n(x)| \leq \frac{M}{(n+1)!} |x-a|^{n+1} \quad (\text{C.4})$$

with  $a = 0$ , where  $\mathbf{M}$  is some value satisfying  $|f^{(n+1)}(x)| \leq M$  on the interval  $I = [a, x]$ . Since we are interested in an upper bound of the error and since  $\mathbf{a}$  is known, we can reformulate the interval as  $I = [0, x_{max}]$ , where

$$x_{max} = \|i\| k_{max} w_{max} h_{max} \quad (\text{C.5})$$

We are interested in computing an error bound for  $e^{ikwh(x,y)}$ . Assuming the following parameters and facts used within Stam's Paper:

- Height of bump: 0.15micro meters
- Width of a bump: 0.5micro meters
- Length of a bump: 1micro meters
- $k = \frac{2\pi}{\lambda}$  is the wavenumber,  $\lambda \in [\lambda_{min}, \lambda_{max}]$  and thus  $k_{max} = \frac{2\pi}{\lambda_{min}}$ . Since  $(u, v, w) = -\omega_i - \omega_r$  and both are unit direction vectors, each component can have a value in range  $[-2, 2]$ .
- for simplification, assume  $[\lambda_{min}, \lambda_{max}] = [400nm, 700nm]$ .

We get:

$$\begin{aligned} x_{max} &= \|i\| * k_{max} * w_{max} * h_{max} \\ &= k_{max} * w_{max} * h_{max} \\ &= 2 * \left( \frac{2\pi}{4 * 10^{-7}m} \right) * 1.5 * 10^{-7} \\ &= 1.5\pi \end{aligned} \quad (\text{C.6})$$

and it follows for our interval  $I = [0, 1.5\pi]$ .

Next we are going to find the value for  $M$ . Since the exponential function is monotonically growing (on the interval  $I$ ) and the derivative of the **exp** function is the exponential function itself, we can find such an  $M$ :

$$\begin{aligned} M &= e^{x_{max}} \\ &= \exp(1.5\pi) \end{aligned}$$

and  $|f^{(n+1)}(x)| \leq M$  holds. With

$$\begin{aligned} |E_n(x_{max})| &\leq \frac{M}{(n+1)!} |x_{max} - a|^{n+1} \\ &= \frac{\exp(1.5\pi) * (1.5\pi)^{n+1}}{(n+1)!} \end{aligned} \quad (\text{C.7})$$

we now can find a value of  $n$  for a given bound, i.e. we can find an value of  $N \in \mathbb{N}$  s.t.  $\frac{\exp(1.5\pi) * (1.5\pi)^{N+1}}{(N+1)!} \leq \epsilon$ . With Octave/Matlab we can see:

- if  $N=20$  then  $\epsilon \approx 2.9950 * 10^{-4}$
- if  $N=25$  then  $\epsilon \approx 8.8150 * 10^{-8}$
- if  $N=30$  then  $\epsilon \approx 1.0050 * 10^{-11}$

With this approach we have that  $\sum_{n=0}^{25} \frac{(ikwh)^n}{n!} \mathcal{F}\{h^n\}(\alpha, \beta)$  is an approximation of  $P(u, v)$  with error  $\epsilon \approx 8.8150 * 10^{-8}$ . This means we can precompute 25 Fourier Transformations in order to approximate  $P(u, v)$  having an error  $\epsilon \approx 8.8150 * 10^{-8}$ .

## C.2 PQ approach

### C.2.1 One dimensional case

Since our series is bounded, we can simplify the right-hand-side of equation 1.38.

Note that  $e^{-ix}$  is a complex number. Every complex number can be written in its polar form, i.e.

$$e^{-ix} = \cos(x) + i\sin(x) \quad (C.8)$$

Using the following trigonometric identities

$$\begin{aligned} \cos(-x) &= \cos(x) \\ \sin(-x) &= -\sin(x) \end{aligned} \quad (C.9)$$

combined with C.8 we can simplify the series 1.38 even further to:

$$\frac{1 - e^{iwT(N+1)}}{1 - e^{-iwT}} = \frac{1 - \cos(wT(N+1)) + i\sin(wT(N+1))}{1 - \cos(wT) + i\sin(wT)} \quad (C.10)$$

Equation C.10 is still a complex number, denoted as  $(p + iq)$ . Generally, every complex number can be written as a fraction of two complex numbers. This implies that the complex number  $(p + iq)$  can be written as  $(p + iq) = \frac{(a+ib)}{(c+id)}$  for any  $(a+ib), (c+id) \neq 0$ . Let us use the following substitutions:

$$\begin{aligned} a &:= 1 - \cos(wT(N+1)) & b &= \sin(wT(N+1)) \\ c &= 1 - \cos(wT) & d &= \sin(wT) \end{aligned} \quad (C.11)$$

Hence, using C.11, it follows

$$\frac{1 - e^{iwT(N+1)}}{1 - e^{-iwT}} = \frac{(a+ib)}{(c+id)} \quad (C.12)$$

By rearranging the terms, it follows  $(a+ib) = (c+id)(p+iq)$  and by multiplying its right hand-side out we get the following system of equations:

$$\begin{aligned} (cp - dq) &= a \\ (dp + cq) &= b \end{aligned} \quad (C.13)$$



After multiplying the first equation of C.13 by  $c$  and the second by  $d$  and then adding them together, we get using the law of distributivity new identities for  $p$  and  $q$ :

$$\begin{aligned} p &= \frac{(ac + bd)}{c^2 + d^2} \\ q &= \frac{(bc + ad)}{c^2 + d^2} \end{aligned} \quad (\text{C.14})$$

Using some trigonometric identities and putting our substitution from C.11 for  $a, b, c, d$  back into the current representation C.14 of  $p$  and  $q$  we will get:

$$\begin{aligned} p &= \frac{1}{2} + \frac{1}{2} \left( \frac{\cos(wTN) - \cos(wT(N+1))}{1 - \cos(wT)} \right) \\ q &= \frac{\sin(wT(N+1)) - \sin(wTN) - \sin(wT)}{2(1 - \cos(wT))} \end{aligned} \quad (\text{C.15})$$

Since we have seen, that  $\sum_{n=0}^N e^{-uwnT}$  is a complex number and can be written as  $(p + iq)$ , we now know an explicit expression for  $p$  and  $q$ . Therefore, the one dimensional inverse Fourier transform of  $S$  is equal:

$$\begin{aligned} \mathcal{F}^{-1}\{S\}(w) &= \mathcal{F}^{-1}\{f\}(w) \sum_{n=0}^N e^{-iwnT} \\ &= (p + iq)\mathcal{F}^{-1}\{f\}(w) \end{aligned} \quad (\text{C.16})$$

### C.2.2 Two dimensional case

$$\begin{aligned} \mathcal{F}^{-1}\{S\}(w_1, w_2) &= \int_{-\infty}^{\infty} \int_{-\infty}^{\infty} \sum_{n_1=0}^{N_1} \sum_{n_2=0}^{N_2} h(x_1 + n_1 T_1, x_2 + n_2 T_2) e^{i w(x_1 + x_2)} dx_1 dx_2 \\ &= \int_{-\infty}^{\infty} \int_{-\infty}^{\infty} \sum_{n_1=0}^{N_1} \sum_{n_2=0}^{N_2} h(y_1, y_2) e^{i w((y_1 - n_1 T_1) + (y_2 + n_2 T_2))} dx_1 dx_2 \\ &= \sum_{n_1=0}^{N_1} \sum_{n_2=0}^{N_2} \int_{-\infty}^{\infty} \int_{-\infty}^{\infty} h(y_1, y_2) e^{i w(y_1 + y_2)} e^{-i w(n_1 T_1 + n_2 T_2)} dy_1 dy_2 \\ &= \sum_{n_1=0}^{N_1} \sum_{n_2=0}^{N_2} e^{-i w(n_1 T_1 + n_2 T_2)} \int_{-\infty}^{\infty} \int_{-\infty}^{\infty} \text{Box}(y_1, y_2) e^{i w(y_1 + y_2)} dy_1 dy_2 \\ &= \left( \sum_{n_1=0}^{N_1} \sum_{n_2=0}^{N_2} e^{-i w(n_1 T_1 + n_2 T_2)} \right) \mathcal{F}^{-1}\{h\}(w_1, w_2) \\ &= \left( \sum_{n_1=0}^{N_1} e^{-i w n_1 T_1} \right) \left( \sum_{n_2=0}^{N_2} e^{-i w n_2 T_2} \right) \mathcal{F}^{-1}\{h\}(w_1, w_2) \\ &= (p_1 + iq_1)(p_2 + iq_2) \mathcal{F}^{-1}\{h\}(w_1, w_2) \\ &= ((p_1 p_2 - q_1 q_2) + i(p_1 q_2 + q_1 p_2)) \mathcal{F}^{-1}\{h\}(w_1, w_2) \\ &= (p + iq) \mathcal{F}_{DFTT}\{h\}(w_1, w_2) \end{aligned} \quad (\text{C.17})$$

Where we have defined

$$\begin{aligned} p &:= (p_1 p_2 - q_1 q_2) \\ q &:= (p_1 p_2 + q_1 q_2) \end{aligned} \tag{C.18}$$

## Appendix D

# Miscellaneous Transformations

### D.1 Fresnel Term - Schlick's approximation

The Fresnel's equations describe the reflection and transmission of electromagnetic waves at an interface. That is, they give the reflection and transmission coefficients for waves parallel and perpendicular to the plane of incidence. Schlick's approximation is a formula for approximating the contribution of the Fresnel term where the specular reflection coefficient  $R$  can be approximated by:

$$R(\theta) = R_0 + (1 - R_0)(1 - \cos \theta)^5 \quad (\text{D.1})$$

and

$$R_0 = \left( \frac{n_1 - n_2}{n_1 + n_2} \right)^2$$

where  $\theta$  is the angle between the viewing direction and the half-angle direction, which is halfway between the incident light direction and the viewing direction, hence  $\cos \theta = (H \cdot V)$ . And  $n_1, n_2$  are the indices of refraction of the two medias at the interface and  $R_0$  is the reflection coefficient for light incoming parallel to the normal (i.e., the value of the Fresnel term when  $\theta = 0$  or minimal reflection). In computer graphics, one of the interfaces is usually air, meaning that  $n_1$  very well can be approximated as 1.

### D.2 Spherical Coordinates and Space Transformation

$$\forall \begin{pmatrix} x \\ y \\ z \end{pmatrix} \in \mathbb{R}^3 : \exists r \in [0, \infty) \exists \phi \in [0, 2\pi] \exists \theta \in [0, \pi] \text{ s.t.}$$

$$\begin{pmatrix} x \\ y \\ z \end{pmatrix} = \begin{pmatrix} r \sin(\theta) \cos(\phi) \\ r \sin(\theta) \sin(\phi) \\ r \cos(\theta) \end{pmatrix}$$

From the definition ?? of  $(u, v, w) = -\omega_i - \omega_r$  and using spherical coordinates *D.2*, we get for  $w$  the following identity:

$$\begin{aligned}
w &= -\omega_i - \omega_r \\
&= -(\omega_i + \omega_r) \\
&= -(\cos(\theta_i) + \cos(\theta_r))
\end{aligned} \tag{D.2}$$

and therefore  $w^2$  is equal  $(\cos(\theta_i) + \cos(\theta_r))^2$ .

### D.3 Tangent Space

The concept of tangentspace-transformation of tangent space is used in order to convert a point between world and tangent space. GLSL fragment shaders require normals and other vertex primitives declared at each pixel point, which mean that we have one normal vector at each texel and the normal vector axis will vary for every texel.

Think of it as a bumpy surface defined on a flat plane. If those normals were declared in the world space coordinate system, we would have to rotate these normals every time the model is rotated, even when just for a small amount. Since the lights, cameras and other objects are usually defined in world space coordinate system, and therefore, when they are involved in an calculation within the fragment shader, we would to have to rotate them as well for every pixel. This would involve almost countless many object to world matrix transformations need to take place at the pixel level. Therefore, instead doing so, we transform all vertex primitives into tangent space within the vertex shader.

To make this point clear an example: Even we would rotate the cube in figure D.1, the tangent space axis will remain aligned with respect to the face. Which practically speaking, will save us from performing many space transformations applied pixel-wise within the fragment shader and instead allows us to perform us the tangentspace transformation of every involved vertex primitive in the vertex-shader.

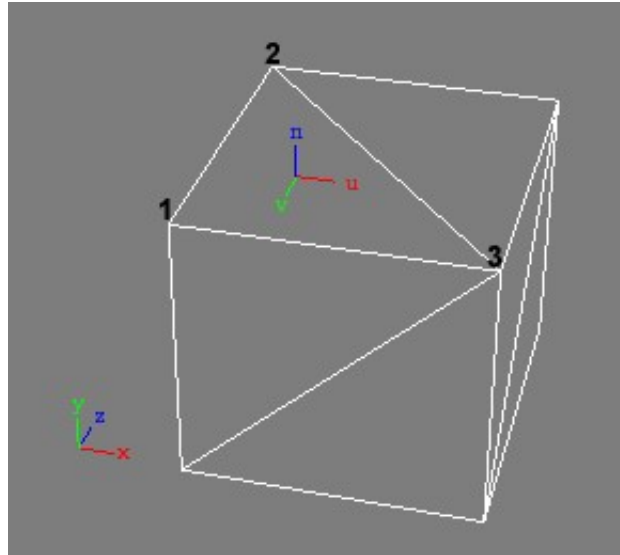


Figure D.1: Cube in world space  $(x, y, z)$  showing the tangent space  $(u, v, n)$  of its face  $(2, 1, 3)$

# List of Tables

A.1 Fourier Transform Mapping . . . . .	38
---	----

# List of Figures

1.1	Problem Statement . . . . .	1
1.2	Problem Statement: Output . . . . .	2
1.3	FT by DTFT . . . . .	3
1.4	Coherence Area using Gaussian Window . . . . .	4
1.5	DTFT by DFT . . . . .	5
1.6	Sinc Interpolation Approximation . . . . .	16
2.1	DFT Terms for a Blazed grating . . . . .	21
2.2	Renderer Architecture . . . . .	22
2.3	Triangular Mesh . . . . .	23
2.4	Camera Coordinate System . . . . .	25
2.5	Camera Matrix . . . . .	25
2.6	Rays of a Directional Light . . . . .	27
2.7	Triangle Rasterization . . . . .	28
2.8	Lookup in DFT Terms . . . . .	32
D.1	Illustration of a Tangent Space . . . . .	48

# List of Algorithms

1	Precomputation: Pseudo code to generate Fourier terms . . . . .	20
2	Vertex diffraction shader pseudo code . . . . .	26
3	Fragment diffraction shader pseudo code . . . . .	30
4	Texture Blending . . . . .	33
5	Sinc interpolation for PQ approach . . . . .	34

# Bibliography

- [Bar07] BARTSCH, Hans-Jochen: *Taschenbuch Mathematischer Formeln*. 21th edition. HASNER, 2007. – ISBN 978–3–8348–1232–2
- [CT12] CUYPERS T., et a.: Reflectance Model for Diffraction. In: *ACM Trans. Graph.* 31, 5 (2012), September
- [DSD14] D. S. DHILLON, et a.: Interactive Diffraction from Biological Nanostructures. In: *EUROGRAPHICS 2014/ M. Paulin and C. Dachsbacher* (2014), January
- [For11] FORSTER, Otto: *Analysis 3*. 6th edition. VIEWEG+TEUBNER, 2011. – ISBN 978–3–8348–1232–2
- [I.N14] I.NEWTON: *Opticks, reprinted*. CreateSpace Independent Publishing Platform, 2014. – ISBN 978–1499151312
- [JG04] JUAN GUARDADO, NVIDIA: Simulating Diffraction. In: *GPU Gems* (2004). <https://developer.nvidia.com/content/gpu-gems-chapter-8-simulating-diffraction>
- [LM95] LEONARD MANDEL, Emil W.: *Optical Coherence and Quantum Optics*. Cambridge University Press, 1995. – ISBN 978–0521417112
- [MT10] MATIN T.R., et a.: Correlating Nanostructures with Function: Structural Colors on the Wings of a Malaysian Bee. (2010), August
- [PAT09] PAUL A. TIPLER, Gene M.: *Physik für Wissenschaftler und Ingenieure*. 6th edition. Spektrum Verlag, 2009. – ISBN 978–3–8274–1945–3
- [PS09] P. SHIRLEY, S. M.: *Fundamentals of Computer Graphics*. 3rd edition. A K Peters, Ltd, 2009. – ISBN 978–1–56881–469–8
- [R.H12] R.HOOKE: *Micrographia, reprinted*. CreateSpace Independent Publishing Platform, 2012. – ISBN 978–1470079031
- [RW11] R. WRIGHT, et a.: *OpenGL SuperBible*. 5th edition. Addison-Wesley, 2011. – ISBN 978–0–32–171261–5
- [Sta99] STAM, J.: Diffraction Shaders. In: *SIGGRAPH 99 Conference Proceedings* (1999), August
- [T.Y07] T.YOUNG: *A course of lectures on natural philosophy and the mechanical arts Volume 1 and 2*. Johnson, 1807, 1807



# **Erklärung**

gemäss Art. 28 Abs. 2 RSL 05

Name/Vorname: .....

Matrikelnummer: .....

Studiengang: .....

Bachelor ☐      Master ☐      Dissertation ☐

Titel der Arbeit: .....

.....

.....

LeiterIn der Arbeit: .....

.....

Ich erkläre hiermit, dass ich diese Arbeit selbständig verfasst und keine anderen als die angegebenen Quellen benutzt habe. Alle Stellen, die wörtlich oder sinngemäss aus Quellen entnommen wurden, habe ich als solche gekennzeichnet. Mir ist bekannt, dass andernfalls der Senat gemäss Artikel 36 Absatz 1 Buchstabe o des Gesetzes vom 5. September 1996 über die Universität zum Entzug des auf Grund dieser Arbeit verliehenen Titels berechtigt ist.

.....

Ort/Datum

.....

Unterschrift